# JKU

## JOHANNES KEPLER
## UNIVERSITY LINZ

Submitted by
**Mgr. Dominik Farka, MSc**

Submitted at
**Linz Institute for Organic Solar Cells (LIOS) Physical Chemistry**

Supervisor and
First Examiner
**o. Univ. Prof. Mag. Dr. DDr. h.c. Niyazi Serdar Sariciftci**

Second Examiner
**Univ. Prof. Dr.[in] Alberta Bonanni**

Co-Supervisor
**DI Dr. Philipp Stadler**

Month Year
IV/2018

# (SEMI-)TRANSPARENT, CONDUCTIVE, METALLIC POLYMERS BY CHEMICAL VAPOUR DEPOSITION

Doctoral Thesis

to obtain the academic degree of

Doktor der Naturwissenschaften

in the Doctoral Program

Naturwissenschaften

JOHANNES
KEPLER
UNIVERSITY LINZ
Altenberger Str. 69
4040 Linz, Austria
www.jku.at

# STATUTORY DECLARATION

I hereby declare that the thesis submitted is my own unaided work, that I have not used other than the sources indicated, and that all direct and indirect sources are acknowledged as references.
This printed thesis is identical with the electronic version submitted.

Linz, 13.4.2018

Signature

# Abstract

Conductive polymers are an established technology with applications reaching from transparent electrodes and active materials for LED's and solar cells to light-weight batteries.

In this thesis, the focus lies with intrinsically doped, (semi-) transparent polymers. The development of a new deposition method based on oxidative chemical vapour deposition (oCVD) and its application to thiophene-based systems is the presented.

The innovation in this process lies with the use of sulphuric acid acting as both, the oxidizing/polymerizing agent and dopant in oCVD. In this way, sulphate ions are integrated into the polymer matrix, leading doping and crystallization in dimensions hitherto unprecedented. Thereby, the small dopant also reduces disorder and in turn promotes extraordinary electron charge-carrier transport properties.

Here, the progress on three thiophene-based polymers is presented: poly(3,4-ethylenedioxythiophene) (PEDOT), poly(3,4-ethylenediothiathiophene) (PEDTT), and poly(thieno[3,4b]pyrazine) (PTP).

PEDOT:sulphate presents the most extraordinary of the three, with a conductivity of more than 4000 S/cm at room temperature and an impressive 3300 S/cm at 1.8 K. It was possible to show, that this polymer operates in the metallic regime of the metal-insulator-transition (MIT) and exhibits MC. Additionally it was possible to measure a Hall effect at low temperature: which is only possible in homogeneous materials of extraordinarily high conductivity and mobility.

The same material was additionally measured in thick-films. In this case, a conductivity minimum and thus a transition to the true metallic state was revealed. The measurements in this system were repeated for high pressures, which resulted in further suppression of disorder and an improvement of electron transport properties.

The second best material, PEDTT:sulphate was an achievement in itself, albeit not as impressive as PEDOT. With 1050 S/cm at room temperature, the previous record from 1995 was beaten 2600-fold. The most impressive about this result is that literature categorically dismissed the material as a good conductive system. In this case, sulphate does not only act as a dopant but also as a structurally stabilizing and disorder-suppressing entity. The material presents a conducting polymer in the critical regime of the MIT.

At last, PTP presents the odd-one out in the series. Though exhibiting interesting properties in the context of adhesion to glass. In the context of conductivity, substantial disorder was detected, partially owed to the unprotected reactive sites apart from the thiophene ring.

# Kurzfassung

Bei leitfähigen Polymeren handelt es sich um eine bereits etablierte Materialklasse deren Anwendungen sich von transparenten Elektroden bis hin zu Aktivmaterialien in LED's und Solarzellen bis hin zu Leichtbau-Batterien erstrecken.

In dieser Arbeit liegt der Fokus auf intrinsisch dotierten, (semi-) transparenten Polymeren. Im Zuge dieser Arbeit wird die Entwicklung einer neuen Methode zum Auftragen von Polymerfilmen, basierend auf oxydativer, chemischer Gasphasenabscheidung (oCVD) und der Anwendung dieser auf Thiophen-basierende Systeme, beschrieben.

Die Innovation dieses Prozesses liegt in der Verwendung von Schwefelsäure als Polymerisationsmittel und Oxidationsmittel bzw. Dotierungsmittel für oCVD. Somit werden Sulfat-Ionen in die Polymermatrix integriert, was zur Dotierung und zu einem geringen Grad an struktureller Unordnung führt. Weiters bewirkt das Sulfat-Ion die Ausbildung von Polymer-Kristalliten beträchtlicher Größe. Auf diese Art und Weise bringt das Dotierungsmittel auch Ordnung in das Material, was wiederum zu außerordentlichen elektrischen Eigenschaften, im Sinne des Ladungsträger-Transportes, führt.

In diese Arbeit werden drei auf Thiophenen basierende Polymere präsentiert: poly-3,4-ethylendioxythiophen (PEDOT), poly-3,4-ethylendiothiathiophen (PEDTT), und poly-thieno[3,4b]pyrazin (PTP).

PEDOT:sulfat stellt das außerordentlichste Material dieser Gruppe dar, mit Leitfähigkeiten im Bereich Jenseits von 4000 S/cm bei Raumtemperatur und 3300 S/cm bei 1.8 K. Im Rahmen der Charakterisierung stellte sich heraus, dass das Material eine sogenannte Metallische Leitfähigkeit und auch eine Magnetoleitfähigkeit aufweist. Außerdem war es bei tiefen Temperaturen (unter 10 K) möglich einen Hall-Effekt zu messen, was nur in Materialien mit einer geringen strukturellen Unordnung, und einer hohen Leitfähigkeit und hohen Ladungsträger-Mobilität möglich ist.

Das selbige Material wurde weiters als freistehender Film charakterisiert. Dieser wies ein Leitfähigkeitsminimum und somit einen Übergang zur "kristallinen" metallischen Leitfähigkeit auf. Messungen unter hydrostatischem Druck zeigten außerdem, dass die Strukturelle Ordnung sich positiv auf den Ladungsträgertransport auswirken.

Das nächste Material ist PEDTT:sulfat, stellt ebenfalls einen großen Fortschritt für das wissenschaftliche Feld dar. Mit einer Leitfähigkeit von 1050 S/cm bei Raumtemperatur wurde der vorliegende Rekord von 1995 um das 2600-fache übertroffen. Die wirklich beeindruckende an diesem Resultat ist, dass die Literatur PEDTT bereits als schlecht leitfähiges Material ohne Aussicht auf Verbesserung abgeschrieben hat. Im Falle von PEDTT:sulfat verringert das Gegen-Ion dank seiner Interaktion mit dem Polymer die strukturelle Unordnung. Das Material liegt im Kritischen Bereich des Metall-Isolator Übergangs (MIT).
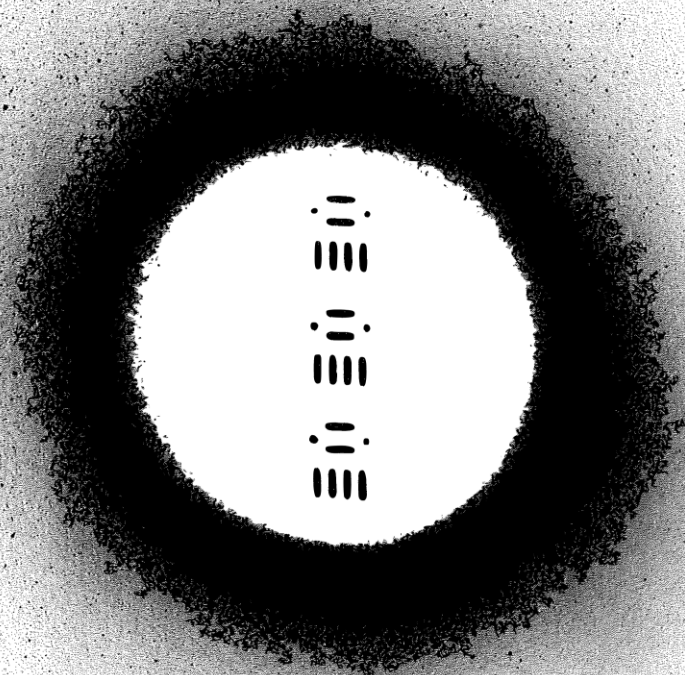
Das dritte Material, PTP, besitzt zwar strukturelle Ähnlichkeit mit PEDOT und PEDTT, seine elektrischen Eigenschaften sind jedoch grundsätzlich verschieden. Es weist teilweise interessante Eigenschaften, wie zum Beispiel eine starke Adhäsion zu Glas, auf. Die Leitfähigkeit bleibt jedoch dank seiner strukturellen Unordnung gering, was direkt von den ungeschützten reaktiven Stellen am Pyrazin-Ring abzuleiten ist.

# (SEMI-)TRANSPARENT CONDUCTIVE, METALLIC POLYMERS BY CHEMICAL VAPOUR DEPOSITION

## Table of Contents

# 1. Words of Praise

Thanks to all, who did me bad,
for I would grow with every step.
Thanks to all who walked with me,
for they would make this thesis be.

With family and friends by side,
I'd cross the blades with things to fright.
My mentors primed me very well,
To conquer and to challenge hell.

With PEDOT in metallic state,
set out to meet the Laureate,
out to discuss, out to present,
sent there by the government.
In Lindau 'twas at Lake Constance,
to meet the future, seize the chance.

Close to the end,
I've crossed the sea,
To find a lab in Berkeley.
New things I found,
Then home-ward bound
Refreshed in spirit as in mind.

Refreshed in spirit,
Refreshed in mind,
Back home to end it,
back home to write.

## 2. Scientific Acknowledgement

## 3. Introduction

Conductive polymers are part of the scientific repertoire since the late 1970's.[1,2] Despite this, there are only few examples of the metallic state being reached.[3–6]

In this thesis, we set out to understand the driving force of the metallic state, where the similarities and the differences between metals and metallic polymers are. To do so, we start with conductive polymer representing the state of the art: PEDOT (poly-3,4-ethylenedioxy thiophene), a well studied system, commercially available, and renown for high conductivities.[7–11] According to multiple groups[11,12], the electronic properties are of a conductive polymer are governed by two parameters, effectively: by its chemical identity and by its disorder. The former can be seen as its intrinsic activation energy. The latter, however, is much more complicated as disorder is not a single parameter. The term disorder relates as much to electronic disorder such as impurities in a silicon lattice, as to structural disorder originating from imperfections in the lattice or grain-boundaries. Very often, however, its exact source cannot be pin-pointed, especially not experimentally, leaving us with treating it as a universal parameter.

Processing of conductive polymers features at least two steps: film deposition and doping. Both present a potential sources of disorder, leaving us with the choice between "cast to dope", which is the typical sample preparation where a deposited film is treated by a doping agent, or "dope to cast", which was only achieved so far in PEDOT:PSS where films are deposited from dispersions of the already doped polymer. The problem remains, that despite achieving highly doped systems, suppression of disorder remains problematic. [11,13–17] We chose the third path of doing everything at once.

To achieve this, we developed a novel approach to oxidative chemical vapour deposition (oCVD), in which we used a hitherto unuknown source of vapour-borne oxidizing agent in the context of oCVD: a mix of sulphuric acid and sodium sulphate.

Compared to other frequently used oxidizing agents such as arsenic trifluoride or antimon pentafluoride it is rather mild. Further, it deposits as sulphate (or hydrogen sulphate), an ion readily forming large crystals and therefore a favourite of Austrian high-school teachers to demonstrate crystal-growth.

In this thesis, we focus on the investigation of electron transport properties of sulphate-doped, oCVD prepared PEDOT and its structural analogues. We investigate conductivity and magnetoconductivity (MC), as well as their further evaluation in the sense of Landau orbit size or Zabrodskii (or W-) plots. In one rare case, we achieved high-enough mobility and film homogeneity to observe a Hall effect in DC measurement.

Electronic properties, however, give no first-hand information on disorder. To monitor that it is necessary to probe optically for the Infra-Red Activated Vibrations (IRAV) bands, investigate the materials chemical or elemental purity, its average chain-length, degree of crystallinity, and many more.

To complement our hypothesis of metallic state, we applied hydrostatic load pressures to further suppress disorder to PEDOT and observe the enhanced properties in a thick film.

Further, we focussed on PEDOT's structural analogues. These were poly- (3,4-ethylenedithia thiophene) (PEDTT) and polythieno pyrazine (PTP). In both polymers the main structure of a thiophene with protecting groups on the 3 and 4 positions remains, the character of the protecting group changes.

The technique was successfully tested and applied to other polymers such as polydopamine[18,19], methylpyrrole*, and other custom made thiophenes* (*unpublished results). In general, thiophenes are easily polymerized and form films, however, making a state-of-the-art polymer requires substantial optimization.

## 4. Materials

Hydrochloric acid (HCl), concentrated, VWR Chemicals
Sulphuric Acid ($H_2SO_4$), concentrated, J.T.Baker
Isopropanol, NormaPUR, VWR Chemicals
Acetone, technical grade, VWR Chemicals
sapphire substrates (C-plane, 0001), CrysTec
diamond paste (1 μm, 0.25 μm)
3,4-ethylene dioxythiophene(EDOT), 99%, Sigma Aldrich
3,4-ethylene dithiathiophene (EDTT), 1-Material Inc.
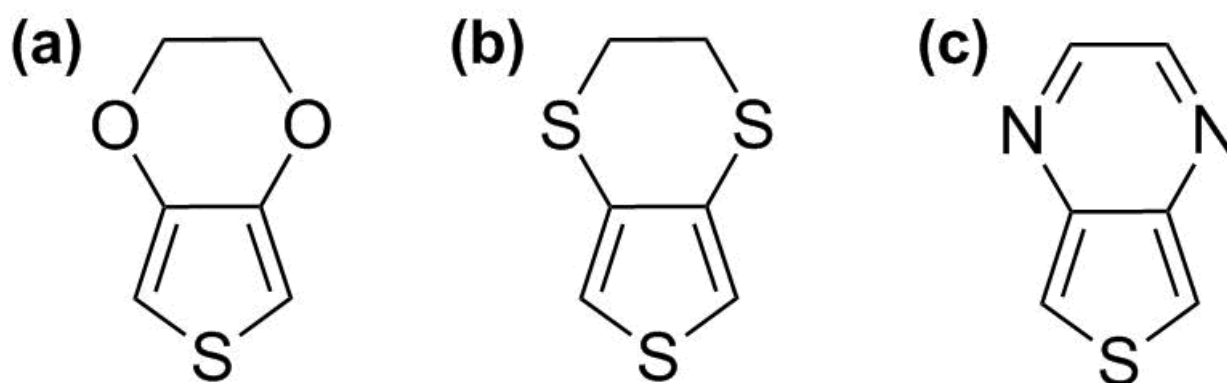thieno[3,4-b]pyrazine, 1-Material Inc.

Figure 1: Monomers used to form materials studies in the scope of this thesis. (a) 3,4-ethylene dioxythiophene(EDOT) (b) 3,4-ethylene dithiathiophene (EDTT) (c) thieno[3,4-b]pyrazine

# 5. Experimental

As a general note, giving a deeper understanding and description for the techniques used during the work on my thesis would be beyond the scope of this work and mostly just a reproduction of existing literature. As a consequence, I will focus in this chapter on good laboratory practices (GLP), specialties of the engines found at this institute and their respective advantages, when multiple instruments of a kind are present. I aim at giving an introduction to the practical aspects that I personally would have found useful for my work.

## 5.1. Sapphire Substrates - use and care

### 5.1.1. Properties

Sapphire ($Al_2O_3$) is an extremely useful material in many ways.
In this thesis, single crystalline sapphire (0001, C-plane) was used, exclusively. The main reason for this is to have the combination of a single crystalline carrier substrate which combines good heat conduction while being electrically insulating. Further, sapphire is chemically inert while one of the hardest materials available, making it an ideal choice in terms of recycling. It can withstand base piranha (used to remove organic residues like conducting polymers), aqua regia (which removes gold), as well as organic solvents in general. Recycling, again, is crucial for reasons of sustainability. (economic and ecological)

### 5.1.2. Evaporating contacts (AlAu, CrAu)

In order to experimentally determine the electrical properties of conducting polymer, evaporation of metallic contacts is necessary. Reasons are, the application of a well known and reproducible electrode geometry as well as to have an interface to the electronics. Typically, contacts are soldered and connected to the electronic measuring device such as the PPMS, the Lakeshore (8400 series) system or a Keithley. (see below)
Contacts may be in general evaporated either on top of the bare substrate or only after applying the conducting polymer. Where the latter is perfectly applicable for PEDOT:PSS, oCVD grown materials studied in the scope of this thesis require evaporation before the application of the conducting polymer. (contact delamination)
Therefore, there are two requirements for the electrode material: It has not only to adhere well to the sapphire substrate, but also withstand the harsh, oxidative environment of the oCVD process. Alternatively, a composite or set of layers may be used. Two metals fulfilling the first condition are Aluminium and Chromium, yet they do not react well to the conditions of the material deposition. On the other hand, Gold contacts do withstand the oxidative environment of the polymer deposition, while they easily delaminate, disqualifying Gold for the purpose.
The solution to this is the combination of Cr/Au or Al/Au, resulting in a well adhering, chemically stable electrical contact-pad.
As mentioned above, a well defined geometry is necessary in order to determine a materials electrical conductivity with as little uncertainty as possible. Therefore, it is crucial to have a set of well defined, high quality evaporation masks available These can be either purchased from a company or made in-house. The in-house workshop can manufacture features as small as 500 µm. (Figure 2) This is directly related to the minimal mask-thickness achievable, which is also 500 µm- below that, mechanical stability of the mask might not be a given. In-house made masks are not suitable for Hall-effect measurements because of misalignment.
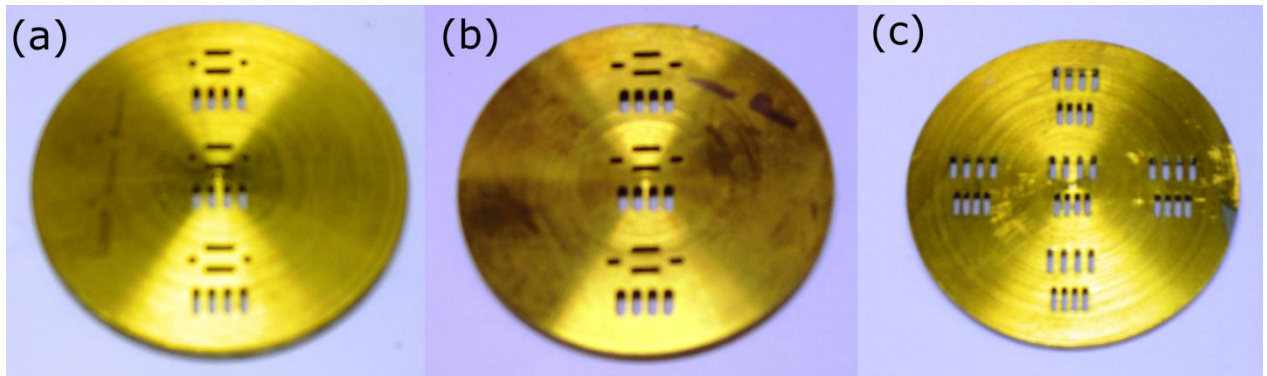
Figure 2: Aluminium-made shadow-masks machined in the in-house workshop. (a) and (b) present the so-called "floppy disc smiley"-design that was intended to combine contacts for Hall and conductivity measurements. The design was later abandoned for insufficient geometrical perfection and replaced by (c), which combined contact distances of 500 and 1000 µm.

As a general recommendation for the design of a new mask would be the use of a 3 mm thick Aluminium disc to convey mechanical stability- the masks must be perfectly flat in order to deliver high-quality contacts! Further, in order to facilitate their use and to make sure a substrate was inserted properly, it is of advantage to have each slot of the same depth as the substrate thickness.

All evaporations for the contact-pads used in this thesis were done in the "Gold Eve" evaporator. Usually, in order to avoid the creation of "shadows" on the substrate, i.e. misalignments of Cr and Au electrode-pad, rotation of the sample is an option. In the case of electrode distances of 1000 µm and less, I recommend avoiding substrate rotation as it can often result in a decrease of electrode distance and discrepancies in geometrical symmetry or in the worst case, an overlap of electrodes.

Instead of rotating the substrates in their mask during their evaporation, place the mask directly in-between two evaporation sources and leave the mask stationary. In this way, the creation of "shadows" is minimized. Therefore, the use of high quality, perfectly flat masks is even more key to success. Alternatively, each of the metal layers can be evaporated one at a time with breaking the vacuum and repositioning the mask after each metal.

At all times, control the quality of the evaporated contacts and the (in-)existance of shadows after each evaporation in order to avoid wrong positive results.

### 5.1.3. Cleaning

#### 5.1.3.1. Removing organic residues (Pyranha)

As mentioned previously, sapphire-substrates must be recycled. A great way to remove organic residues such as silver-paste, conductive polymers, and others, is the use of base piranha. A beaker of 300 mL deionised water is heated to 80 °C and 5 mL of $NH_4OH$ are added. Sonication for ca. 15 minutes removes most organics and can delaminate badly evaporated metal-contacts. The total volume should be changed to fit your personal requirements.

A more aggressive version can be achieved by replacing the aqueous ammonia by sodium hydroxide or potassium hydroxide- this should not be needed in the regular case.

#### 5.1.3.2. Removing contacts (Abrasive)

Removal of contacts can prove a rather challenging endeavour. The first reason is, that the materials used here are chosen in a way to withstand vapours of sulphuric acid- harsh, oxidative conditions in themselves.

One way how to achieve this, is the use of abrasives. A general recommendation is the use of sanding paper in the first place in order to remove organic residues and macroscopic features.

Then, abrasion-polishing using diamond paste (1 µm, 0.25 µm) is performed. For this, a small amount of paste is applied to a special pad and each substrate is polished in circular motion until the contacts are not visible anymore. The smaller grain size should be used only as a last, short polishing step.

After using diamond paste, it is necessary to remove organic residues by an apolar, aprotic solvent such as acetone or toluene. Sonication of a soxhlet apparatus are necessary.

Alternatively, a slowly-spinning spin-coater specifically modified for that purpose can be used to speed-up the process - with the increased shear-rate you can replace diamond paste with tooth paste as it contains alumina and titania which works just as well. (personal communication Stepan Demchyshyn) Rinsing with water and polishing by dust-free fabric are required to remove any residues from the process.

Polishing with one of the above methods represents the only resort if the sapphire substrates got chemically damaged or roughened. This typically happens when the substrates were heated to elevated temperatures (>300°C) and manifests in a milky surface after chemical removal of contacts.

### 5.1.3.3.    Removing contacts (chemically)

Chemists are often said to try and avoid manual work given half a chance- especially concerning cleaning. At least in the latter I would not disagree. Gold and many other metals can be easily etched in aqua regia. In the case of Chromium, however, things are more complicated. In the event of oxidation, a stable oxide layer forms on top of the metal, effectively stopping any more damage to occur to the bulk of the metal. Therefore, etching is best done in a medium that which can reduce the protective oxide layer and dissolve the underlying metal. The way typically relied upon is the use of Chromium etch (6% Nitric Acid in aqueous 16% Ceric Ammonium Nitrate)

In our case, similar yet different method was chosen as it can be prepared from chemicals found in most laboratories. After immersing the substrates in dilute HCl (1:1 in deionized water), add a spatula of Zinc powder. Herein, the Zn-powder acts as a reducing agent while the diluted acid dissolves the underlying chromium. Using the proper concentration will remove even several nm thick layers in a few seconds, leaving the sapphire substrate intact.

## 5.2. Oxidative Chemical Vapour Deposition (oCVD)

### 5.2.1. CVD - power and limitations

CVD is a powerful technique for the synthesis of conducting polymers as it opens up entirely new possibilities as well as deliver materials of high quality in a fast and reproducible way.[20] An alternative name of CVD of polymers is vapour phase polymerization (VPP).

An extensive introduction to CVD in general can be found elsewhere.[21,22] As a basis, CVD will always feature two things: a monomer and an initiator of the polymerization reaction. The former is in all cases encountered supplied in the form of its vapour, while the latter can be a chemical pre-coated onto the substrate or supplied in the vapour phase. Also, plasma can be used as an initiator. An interesting application of CVD was done by Cho and co-workers.[23] By pre-coating the substrate with the oxidant and applying a nano-pattern (in this case lines) the creation of PEDOT-based nanowires was possible. The therein presented the electrode-distance dependence of the conductivity indicates the creation of a topological insulator.[24]

The biggest strength of CVD is equally its biggest drawback. In CVD, the reactions constituents must pass through the vapour phase- the only exception are the cases, where the reaction initiator is pre-coated onto the surface. Therefore, any non-volatile reactant will not participate in the reaction, leading to an intrinsic purification step and a minimization of the human error. Non-volatile contaminations such as metallic impurities in the polymer matrix are limited, and in our case, can be categorically excluded. The reaction ratio's in the herein presented reactions are governed purely by thermodynamics: the chemicals vapour pressure, over-temperature, and gas flow.

Unfortunately, bringing chemicals to the vapour phase presents an intrinsic limitation. Tuning evaporation- or sublimation-rates of all reactants is crucial but complex. For the use of non-volatile constituents (*i.e.* oxidants) certain "tricks" have to be developed and applied.

Most monomers are non-problematic. They can be introduced into the gas-flow by simple bubbling or heating within the furnace to sublime or evaporate. In our case, as we use oCVD, we needed an oxidant that is volatile enough yet readily available, non-toxic, and abundant. We have tried various methods ranging from oleum (fuming sulphuric acid), over sodium hydrogen sulphate ($NaHSO_4$) to mixtures of sulphuric acid ($H_2SO_4$) with sodium sulphate ($Na_2SO_4$), revealing that a 1:1 weight ratio suits our purpose best. Where other oxidants possibly over-oxidize the material, the oxidant forming from the salt-acid mixture doesn't. As the boiling point of sulphuric acid lies well above our process temperature, we assume that the mixture of acid and $SO_3$ is generated, both polymerizing and doping the resulting polymer.

When the polymerization occurs, another advantage of oCVD comes into play. As the polymer forms and the reaction volume cools down at the end of the furnace, the polymer precipitates from the vapour phase and is deposited on a substrate. Just like in gas chromatography, different materials will be resolved and will be deposited at different positions. This intrinsic purification step allows the experimentalist to choose the best fraction and optimize the process accordingly. Thus, even relatively low-purity monomers can result in highly conducting films.

### 5.2.2. Maintenance of the glass tube reactor

As the glassware used in CVD will be heated to hundreds of centigrade, even minor organic residues like grease from fingertips can lead to significant damage. The rules given below were obtained from personal communication with Mr. Mausz, our glassblower-master. Following these, increased glassware-lifespan for tube reactors was observed. Prior to that or in the case of neglect, a rapid deterioration of glassware and brittleness resulted. Especially breaking of the mechanically strained tube-ends was a common issue.

First, the glass tubes used for our CVD setup are most vulnerable at their edges. Therefore wrap these in a layer of insulation-tape. Colour code your tape in order to immediately distinguish glass from quartz. We used grey for glass, blue for quartz. (Figure 2; colours and edge colours) To distinguish these in the first place, look at the edge of the tube, along its length. Quartz will have a pure, pristine-white colour whereas glass will have a green tinge to it.

Second, never put the glass tubes under stress after they were heated up. While hot or even just warm, they are extremely sensitive to mechanical stress and will break. Glass can be easily replaced or cut back. Quartz is significantly more expensive and brittle: what glass can easily survive will break quartz to pieces. Therefore, avoid mechanical cleaning like scrubbing or similar if possible. (details below)

Third, when hot, organic residues on a glass or quartz tube will start to react with the surface and infiltrate the material, turning it from translucent to milky and even more brittle. Parts of the tubes directly exposed to the heat of the furnace should never be touched by gloves and especially not by bare hands as the bodily grease is especially reactive towards glass when heated.

Of course, during cleaning contact to the tubes cannot be avoided. During that, use nitrile gloves while cleaning glass tubes. A simple scrubbing with regular detergent and tap water can be applied. After scrubbing, rinse each tube with ca. 400 mL of tap water ( when the soap-bubbles are not be visible anymore, rinse with ca. 100 mL), followed by ca. 200 mL of deionized water. After drying the outsides of the tube with a regular paper-tissue, rinse the insides with isopropanol and let dry in air.

As stated above, For quartz, manual stress should be avoided at all times. Apply the procedure described in the preceding paragraph only as choice of a last resort. In that case, put a sponge underneath the tube to decrease mechanical stress. Otherwise, assemble the oven as for synthesis and insert a vial containing ca. 1 mL of $H_2O_2$ into the tube. Heat to 200 °C in a nitrogen-gas flow for 30 min or until any visible "dirt" disappears (+10 min).

### 5.2.3. Synthesis

For synthesis of the materials presented in this thesis, the same procedure was used, with some variations. In this paragraph, I will focus solely on assembly of the furnace and insertion of chemicals. Peculiarities for each of the two ovens at our disposal will be described separate paragraphs shown below. Figure 3 shows a graphical summary of the synthesis process, synthesis details, and some achievements.
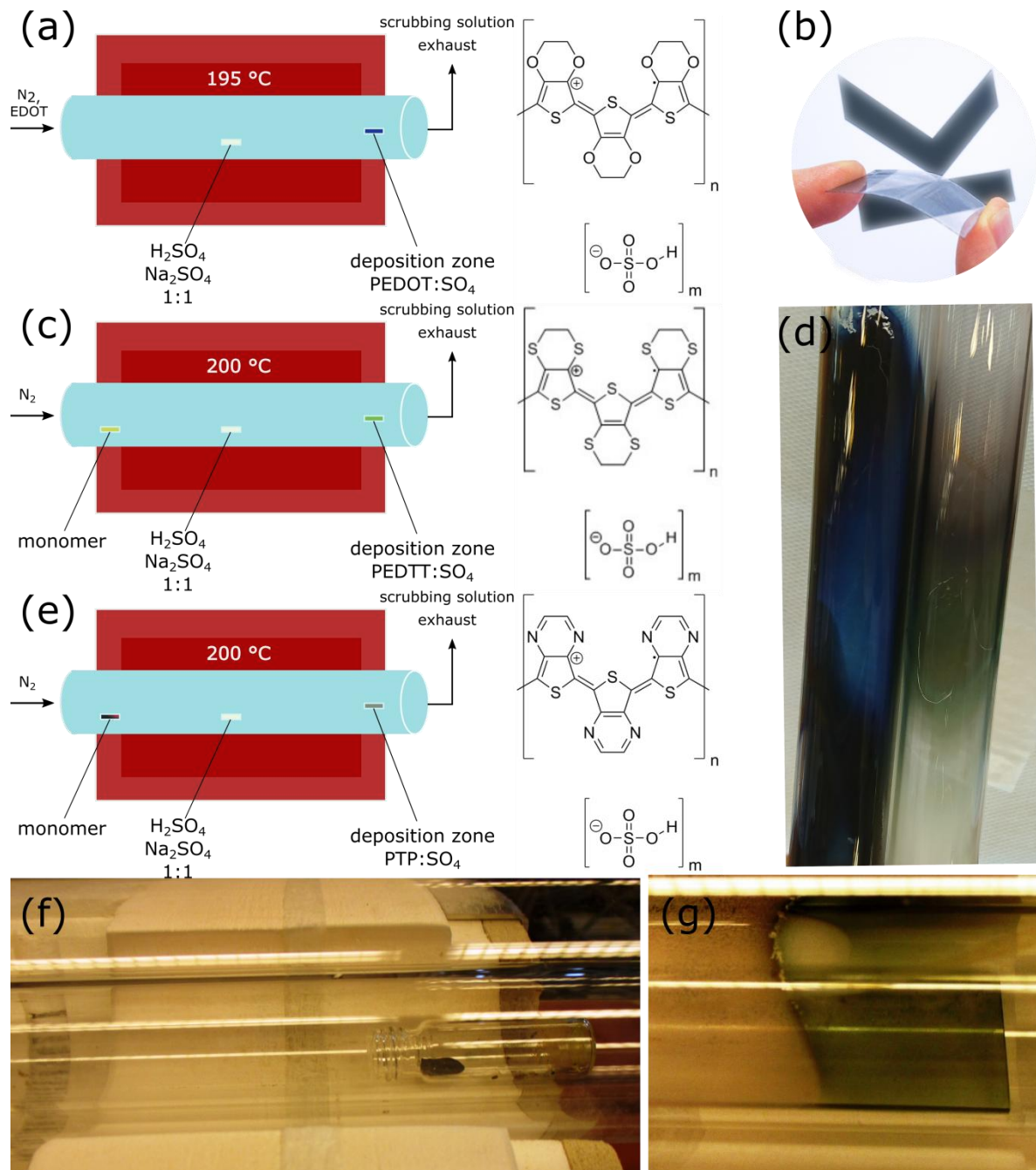
Figure 3:(a) Synthesis assembly of the tube reactor and chemical representation of PEDOT:sulphate. (b) PEDOT:sulphate on mica substrate- the material remains conductive after bending the substrate. (c) Synthesis assembly of the tube reactor and chemical representation of PEDTT:sulphate. (d) Comparison of oCVD-grown PEDOT and PEDTT in the tube-reactors. (e) Synthesis assembly of the tube reactor and chemical representation of PEDOT:sulphate. (f) Positioning of monomer for PTP-synthesis. Accurate positioning is key to success and is one of the few sources of human error in this synthesis. For PEDTT, the monomer needs to be moved closer to the heated zone whereas for PEDOT, heating is counter-productive. (g) PTP within the tube furnace.

### 5.2.3.1. Preparations and assembly

Assembly of the tube reactor for oCVD requires the insertion of three things into the tube: the oxidant, the monomer, and the substrate holder with substrates. (Figure 3a,c,e) In Figure 3, schematic representations of the furnace assembly for the synthesis of the herein presented CP's can be viewed.

Starting with the oxidant, weigh ca. 500 mg of $Na_2SO_4$ into a 4 mL glass vial. Lay the vial flat and distribute the powder or the crystals evenly. Then, add ca. 500 mL of sulphuric acid. The exact amount is not of importance. The synthesis, however, was optimized for values between 500 and 700 mg of salt mixed with the same amount (in mL) of acid: for instance, 536 mg of salt would mean 535 mL of sulphuric acid have to be added.

For the substrate holder, use a glass slide typically used for microscopy and cut it to the needed size. A tube diameter of 25 mm will require glass slides of 22-23 mm in width. (since they are not of infinite thickness) This results in the substrates being positioned in the middle of the tube or lower. For tube-diameters of up to 30 mm this is not an issue- for larger diameters it is as the deposition rate on the substrates drops significantly. (especially true for the 50 mm tube used in the Nabertherm furnace)

Because of the harsh conditions within the tube furnace, the choice of possible substrates is limited. Mind that the substrate must fulfil two conditions (for the syntheses presented here): heat stability above 200 °C combined with chemical stability against acids and oxidative conditions. Here, I present a list of substrates used during my work.

Possible substrates are: glass, sapphire, gold (evaporated on glass or sapphire, with and without adhesion layer), mica (flexible substrate), fluorine-doped tin oxide (FTO, on glass), carbon felt.

Substrate-materials that failed are for either melting or chemical instability were: Indium-tin oxide (ITO, on glass), freestanding foils of PE, PET, polycarbonate, Kapton tape, and many more typically used structural polymers. So far, no insulating polymer was found that could withstand the synthesis-conditions and deliver a conducting film.

The list of tried materials is additionally presented in table 1.

| Material | CVD suitability | Material | CVD suitability |
|---|---|---|---|
| **Glass** | Yes | ITO | No |
| **FTO** | Yes | PE | No |
| **Sapphire** | Yes | PET | No |
| **Mica** | Yes | Polycarbonate | No |
| **Gold** | Yes | Kapton | No |
| **Carbon felt** | Yes | | |

Table 1: List of materials tested for general compatibility with oCVD process.

### 5.2.3.2. Carbolite company furnace - "Old" Furnace

Both furnaces, old and new, have their advantages and disadvantages. The tube furnace by the Carbolite-company scores in simplicity and adaptability. Electronically, temperature can be adjusted *in-situ*. Further, liquid monomers can be introduced by bubbling.

However, this system lacks any type of automatisation or programming-possibilities making it ideal for prototyping or for schooling of students. An substantial drawback of the system is the construction of the furnace: in order to remove the tube reactor, the reactor has to be opened and extracted from the side of the furnace. An substantial advantage of the furnace is the light-weight and compact build of the system. This makes it possible to move the engine to a different place, for instance into a fume hood, possible. That opens up the possibility to work with hazardous materials. Some core parameters can be found in table 2.

| Parameter | Range |
|---|---|
| Temperature range | 0-1200 °C (tube material!) |
| Gas Flow | 0-5 L min$^{-1}$ |
| Tube diameter | Up to 30 mm |
| Opening possible? | NO |
| Moving possible? | YES |
| Bubbling | YES |
| Programming | NO |
| In-situ control | YES |
| Reproducibility | MEDIOCRE |

Table 2: Carbolite tube furnace hard facts.

### 5.2.3.3. Nabertherm company furnace -"New" furnace

The Nabertherm furnace, internally referred to as the "new" furnace, is ideal to produce materials on publication quality. Once optimized, the material can be made reproducibility, quickly, and without the danger of exposing the material to air when there is the need to quickly cool the tube reactor. Further, as opening of the heating part during the reaction is possible, monitoring of the reaction *in-situ* does not present an obstruction. As a recommendation to further students, a somewhat optimized material should not be synthesized in any other furnace than this.

The 50 mm quartz tube supplied with the furnace can withstand the maximum temperature of the furnace. Also, this tube fits the furnace diameter perfectly, allowing excellent temperature control within the furnace. For the reaction, however, a diameter of 50 mm is not ideal and would require the use of a special substrate holder as the most reactive gas-mixture typically accumulates on the upper part of the furnace. As making a custom glass holder out of glass (or quartz) presents a problem, the solution lay in the use of a double-tube system. The 50 mm tube acts as a sheath for a tube of smaller diameter (*i.e.* 25 mm) which acts as the reaction chamber. Thus the reactive vapours accumulate in the height where the substrates are positioned and films can be grown reproducibly. In principle, contamination of the "sheath" is possible, yet negligible. Also, this makes it possible to run quick successions of syntheses where only the reaction tube has to be exchanged. Thus, the quartz tube is exposed to less mechanical stress and its lifetime is expanded.

| Parameter | Range |
|---|---|
| **Temperature range** | 0-1100 °C (mind tube material!) |
| **Gas Flow** | 0-600 L $h^{-1}$ (supply limited) |
| **Tube diameter** | Up to 50 mm; double-tube possible |
| **Opening possible?** | YES |
| **Moving possible?** | NO |
| **Bubbling** | NO |
| **Programming** | YES |
| **In-situ control** | Limited |
| **Reproducibility** | High |

Table 3: Nabertherm tube furnace parameters.

### 5.2.3.4. Synthesis parameters

In the tables below, the synthesis parameters for the polymers tested can be found. Changing a tube furnace is a non-trivial process. Substantial recalibration might be necessary and limitations might apply that were not found in other engines.

PEDOT:sulphate was grown in both the Carbolite furnace as well as the Nabertherm furnace. The respective parameters can be found in tables 4 and 5.

| Thickness/ nm | Carrier gas flow ($N_2$) / L $h^{-1}$ | Reaction time/ s |
|---|---|---|
| **7** | 83 | 180 |
| **10** | 16 | 900 |
| **155** | 16 | 4500 |
| **250** | 83 | 920 |
| **171,000** | 83 | 57600 |

Table 4: Parameters for the growth of oCVD PEDOT:sulphate grown in the Carbolite furnace at 200 °C with ca. 1 g of oxidizing agent added to the solution and saturated EDOT vapour. Note, that there is not always a linear relationship between growth time.

The Nabertherm-furnace is programmable and offers the use of 3 different temperatures zones. Typically, the zone offsets in flow direction were set to -80, 0, and -20 K from the set-temperature of the relative programme step, i.e. a set temperature of 200 °C would mean 120, 200, and 180 °C being exerted by the heating elements in the different zones.

The programmability would allow for breaking down the synthesis into different phases: a ramping of the heating process (with starting and ending temperatures given) and a holding time of said T. Cooling would occur by air-only. It is in theory possible to enhance cooling by opening the furnace, however, I do not recommend this as large deviations in material quality between batches would result. The programmes were optimized for material quality.

The furnace requires the use of a tube of a diameter of 5 cm for optimal heating performance. To reach optimal deposition rates and material use, a second tube was inserted into the primary tube, acting as the actual reactor.

| Thickness / nm | Heating ramp | Holding step |
|---|---|---|
| **43** | 15 min, 25-195 °C | 5 min, 195 °C |
| **350** | 15 min, 25-195 °C | 30 min, 195 °C |

Table 5: Growth parameters for PEDOT:sulphate for the Nabertherm furnace (80 L/h carrirer gas flow, monomer placed into the tube but before the heated zone for optimal vapour concentration)

The growth parameters for PEDTT can be found in table 6. Note, that a gradual slowing of the deposition rate occurred. A reuse of the monomer was possible, yielding similar deposition rates.

| Thickness / nm | Heating ramp | Holding step |
|---|---|---|
| 26 | 20 min, 25-200 °C | 5 min, 200 °C |
| 60 | 40 min, 25-200 °C | 45 min, 200 °C |
| 400 | 40 min, 25-200 °C | 105 min, 200 °C |

Table 6: Growth parameters for PEDTT:sulphate for the Nabertherm furnace (80 L/h carrirer gas flow, monomer placed into the tube at the entrance to the furnace, yet before the first heated zone for optimal vapour concentration)

Growth parameters for PTP are given in table 7. The combination of thermal instability and low vapour pressure of the materials meant that all materials used would have to be disposed after one synthesis. Only limited thicknesses were achievable.

| Thickness / nm | Heating ramp | Holding step |
|---|---|---|
| 10 | 15 min, 25-180 °C | 10 min, 180 °C |
| 56 | 40 min, 25-200 °C | 45 min, 200 °C |

Table 7: Growth parameters for PTP:sulphate for the Nabertherm furnace (80 L/h carrirer gas flow, monomer placed into the tube at the entrance to the furnace, yet before the first heated zone for optimal vapour concentration)

Further, the choice of substrate resulted in significantly different deposition rates and material quality. The thickness in table 4 is given for sapphire. Glass or gold would show several hundred nanometres thicker layers. The material deposited on top of gold would show similar 2-point resistances as the material on top of .

A graphical representation of the growth-setup used for different polymers can be found in Figure 4.

## 5.3. Physical Property Measurement System (PPMS) - peculiarities and related GLP

### 5.3.1. Contacting

An electrical contact is more than just putting a wire on top of a material, but needs to be proper and well done. As described above, a metal-pad needs to be evaporated, if sapphire substrates are used. Then, solder a drop of indium on top the wire to be contacted. Now, when the indium-enveloped wire is pressed, i.e. by tweezers, on top of the metal pad, a contact should be established. Verify the stability of the contact by gently pulling on the wire. A good contact will withstand the mechanical stress- if it wouldn't, it likewise wouldn't withstand the stress of cooling to temperatures below 2 K and therefore ruin the subsequent measurement.

If you cannot establish a contact, there are two most frequent reasons: delamination of the contacts and instability of the indium-metal-pad contact.

In the former case, you can try and remake the contact on a different part of the pad. However, in this case you will only be able to deduce a temperature-conductivity profile, not any value you receive will be meaningless as you lose the geometric information. In most cases, contact delamination means you will have to remake the samples from scratch, taking better care when cleaning the substrates. (base piranha!)

In the latter case, try the use of rosin (Kolophonium). This is the same as when soldering regular tin.

Alternatively, when the pressure cell is used, you can contact the sample boards using indium. However, if you measure a freestanding film, the use of highly-viscous silver-paste is necessary. Apply a small droplet to each contact pad and work quickly. Then, put the flake of material on

top and make sure that no excess silver paste covers the flake- this would interfere with your measurement.

When done, in both cases, use a multi-meter to assure you have established an ohmic contact. To avoid damage done to the sample, i.e. due to stretching, put the PPMS sample puck to the user-bridge and check via its sockets. A linear resistance-distance relationship should be observed. This is, unless you expect to have a topological insulator, which should result in an exponential behaviour.

From time to time, it is necessary to replace the wires connecting the PPMS sample puck to the sample. In the case of the pressure cell, you will have to do this each time you use the cell. First, only use very thin silver wires (> 1 mm in diameter) to prevent contact-breaking due to tension in the wire. Second, use only tin for soldering. Sometimes, the tip doesn't interact well with the tin. In this case, use sanding paper to remove any dirt, followed by a bit of rosin. This will result in the removal of any grease and simplify your work.

Then, put the wire on top of the puck-pad to be contacted and press the solder-head on top. Quickly remove the soldering iron the moment the tin melts. Residual grease will mean you will have to heat wire and pad for a longer period of time. This should result in a "rock solid" contact that can withstand even rough manipulation. The weak point of the contact is the mechanical stability of the silver wire.

When done, use a multi-meter to assure you haven't accidentally contacted the pads in-between each other.

### 5.3.2. Pressure Cell

The pressure cell for the PPMS ETO-option is a rare piece of equipment. Utilizing a CuBe alloy, magnetic fields can penetrate the cell and interact with the sample. The pressure is applied using a hydraulic press and held in place by screwing the caps tight.

Detailed information about its operation can be found in the manual, which is why I will point out only the most important things to keep in mind.

Concerning the sample, special sample boards are supplied by the manufacturer. These sample boards allow synthesis directly on top of them (PEDOT and PEDTT), even in the conditions present in the tube furnace. Alternatively, a freestanding film can be mounted with great care on top of the board using silver paste. The former method is limited to air-stable materials and such, that do not inhibit the synthesis. Air-stability is crucial, as the sample board needs to be contacted afterwards to the wires connecting the cell to the PPMS. The latter way can be used for any kind of material which you can create a freestanding film from.

Contacting the sample boards was typically done by the technician of the Institute of Applied Physics, Mr. Nimmervoll, as great skill and equipment is necessary. Contacting via indium soldering is also possible and was performed, however, requires an absolutely clean sample board to begin with as well as a calm hand and good equipment.

Once contacted, another crucial step happens: insertion into the pressure cell. Once the sample leads are threaded through a tiny hole in the lower cap and the sample is immersed in the teflon cap filled with Daphne 7373 oil (see manual for details!), the cap can be screwed to the pressure cell main body. Take special care to fully screw the cap inside. Failing to do so might cause damage to the sample leads during pressurization and results in failure of the experiment.

Another word of caution concerns maximum pressure. Never exceed the maximum pressure of 3 GPa, as it might result in permanent damage to the cell!

Depressurization of the cell is the probably intellectually most challenging part of the whole process as it is for most counter-intuitive. Therefore, follow the instructions below:

1. After pressurizing the cell, leave the top screw in place. (do not turn it!)

2. After finishing your measurement, assemble the cell as for pressurization and lift the pressurizing dish up by pulling the lever until the previously applied pressure is reached.

3. Now, release the pressure by unwinding the top screw cap. Gently release the pressure and continue in the opposite way as when applying the pressure until you reduce the applied pressure to 0.

4. After you disassemble the pressure cell, the teflon cap as well as the alloy-rings enclosing it will typically remain stuck in the cell. If they put up too much resistance, try to gently tap on the back of the removal tool (see manual) using a small hammer or a wrench. This is necessary as the elevated pressure and release of superfluous oil significantly increases friction.

The procedure can be also found in the pressure-cell manual.

### 5.3.3. Measurement

The PPMS is capable of long term programmes. In general, you will be using the ETO option, which has no limitations, time-wise, and several days long sequences can be run. As a general note, follow the advice in the application notes and manual.

First, however, a short introduction. The PPMS is capable of measurements in a temperature range from 1.8-400 K. (working in conductive polymers, you will rarely rely on temperatures above room temperature) Thanks to the integration of a superconducting magnet, fields from +/- 9 T are accessible. The peculiarities of such magnets, i.e. residual fields, are more important for vibrating sample magnetometry (VSM) and magnetic property measurements in general and will not be described any further.

However, there are some peculiarities with conductivity measurements at low temperatures. At temperatures below 10 K, Joule heating, that is heating due to the conduction of carriers, can become an issue. This would result in heating effects, i.e. an increase of temperature despite the systems attempts cooling, effecting an increase of conductivity. The current cooling power can be read in the CryoMon menu in the PPMS. This value must be at all times significantly higher than the Joule heating power ($P_{Joule} \sim R^2 \cdot I$)

When the temperature of interest lies below 4 K, helium is not quite enough to ensure cooling. Therefore, so called Helium-3 ($^3_2He$) is separated from Helium-4 and used for cooling. Thus, any issue with loss of cooling power below 4 K might be related to an issue with Helium separation (or a software-bug). Contact the master user or the company Quantum Design-LOT.

In general, before exporting your result data, take a close look at the temperature section of your measurement, especially for high resistivity samples. If the temperature is not perfectly constant, be cautious.

Another important parameter to take into account is the phase of the voltage. This should be ideally constant and 0. Some samples show a non-zero, yet unchanging, phase shift. These results can be considered as valid. In some samples, a variation of the phase shift can be observed, typically occurring in tandem with an inexplicable change in conductance behaviour. These results shall be treated as false and the measurement needs to be repeated, with remade contacts or a fresh sample.

A last point of care has to be taken in the choice of electrode geometry used in conductivity measurements. Albeit powerful, the system is not made to cope with a van-der-Pauw (vdP) geometry and only 4-probe geometries are applicable. The use of vdP-geometry outside of Hall measurements typically results in a phase-change at low T. The only way how to make use of a vdP-geometry for conductivity measurements is the addition of current-contacts on the edges of the sample. (Figure 4)
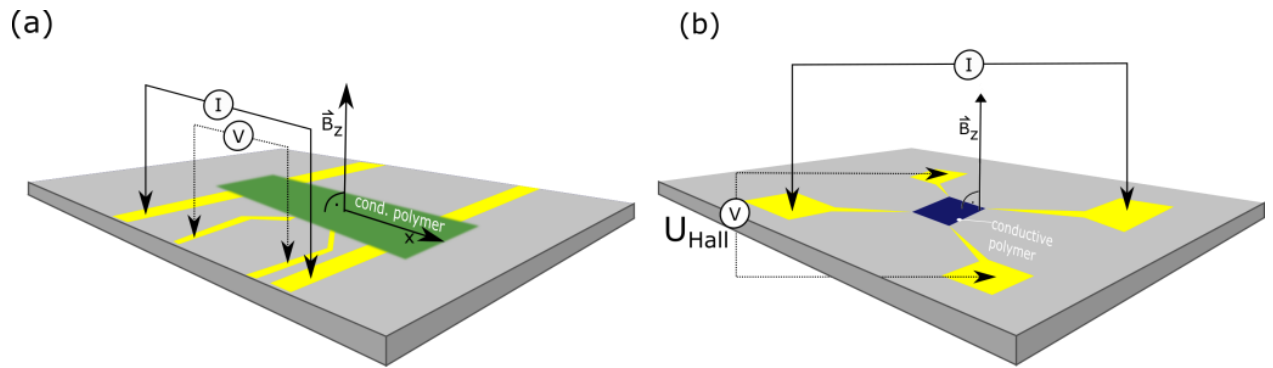
Figure 4: Geometries for measurements in PPMS. (a) 4-probe measurement used for (magneto)-conductivity. A current is applied between the outer contacts, the voltage drop is observed between the inner contacts, thus eliminating parasitic (contact) resistances. (b) Van-der-Pauw contact geometry used for the determination of Hall voltage. The magnetic field should deflect charge carriers moving from the current-leads according to their charge: based on the Lorentz force, it is possible to identify the majority charge carriers to be either electrons and holes.

Further, for more underscore{experienced users}, I recommend the installation of Team-View software to have access to your experiment even when not on-site. This enables you to monitor your experiment from home, during travels, and weekends. Further, it allows making changes to a running programme when an error was done during writing the programme code. Exceeding the compliance limit is a typical example, repetition of a measurement part where a phase shift occurs is another one. Mind, that in order to use the full power of external excess, you need to have a stable, well working sample. If you prepare a sample for a weekend-run or before a conference/vacation, do so already a day in advance and have a second sample ready to have plenty of time to fix minor errors during contacting, etc.

### 5.4. Lakeshore system - peculiarities and related GLP

#### 5.4.1. Contacting

For contacting, all the same rules apply as for the PPMS systems. (see chapter 5.3.1)

#### 5.4.2. Measurement

The Lakeshore system (8400 series, featuring an electromagnet) has distinct advantages over the PPMS system, yet also some limitations.

First, only vdP contact symmetries are applicable. Further, and most important is the distinct limitation of the temperature (ca. 10-300 K) and magnetic field (ca. 0-1 T). The latter limitation is due to the use of a regular electromagnet over a superconducting one. Another peculiarity is the working principle of the cooling system. The default temperature is equivalent to the minimal temperature. Higher temperatures during measurement are reached by constant cooling while the sample is heated. When exchanging a sample, the system cooling needs to be turned off and heated to room temperature to avoid trapping of water.

The possible biggest advantage of the Lakeshore, concerning conductivity measurements, is the significant reduction of human and experimental error originating from geometry. By internally switching the contact configuration, artefacts coming from contact misalignments, altered contact geometry, and sample inhomogeneity are eliminated. Thus, thickness becomes the most and virtually only relevant parameter. This, can be easily measured, i.e. by profilometry.

As vdP geometries are used, Hall measurements can be easily conducted without exchanging the sample.

Another advantage of this system is the availability of the AC Hall measurement, where the magnetic field is oscillated during measurement. Details to this technique can be found in the engines manual and will not be discussed further.

### 5.5. UV-vis

For a chemist (or a biologist!), UV-vis spectroscopy is one of the most common and trivial ways of analyzing a sample.[25] Therefore, I will just focus on the peculiarities of measuring solid samples, as I can safely assume basic knowledge with measuring solutions.

In general, the same rules apply. A jet-black sample will not allow light to penetrate- where in solution analysis a decrease in concentration would be sensible, a decrease in sample thickness is recommended in the measurement of films. Further, instead of measuring in dependence of concentration, only path length is relevant, therefore knowledge of the sample thickness is crucial and should be always stated.

Experimentally, the differences are higher in number. First, the blank should be always a clean substrate of choice, in most cases glass. Further, it is not enough to measure transmittance as a samples reflective properties might play a role. For this, a working knowledge about optical elements is of advantage.

First, the measurement of reflectance proves more challenging than the insertion of a sample-filled cuvette. For the results presented herein, the samples were measured by being placed on top of special mount that is based on the use of a prism. Another method would be the use of an integrating sphere.

Second, when an integrating sphere was not used, the choice of mirror is crucial. Keep in mind, that every mirror has its own reflective properties and that these might differ, especially in the non-visible regions. A good example is the mirror located in the drawer next to our Perkin Elmer UV-vis spectrometer (Lambda 1050). As it is an Aluminium-coated mirror, a decrease in

reflectance in the near IR will be observed. Before designing an experiment, it is wise to consult the webpage of a manufacturer of optical elements, i.e. Thor Labs to avoid unnecessary errors. To get a feeling about the mirror's properties, a clean glass slide should be always measured additionally. As a result, an almost constant reflectance of ca. 6-10% is expected. (depending on quality and cleanness)

Another challenge is found when the sample or mirror is placed onto the mount. First, set the wavelength to the green region, for instance 525 nm, and darken the room (possibly turn off screens, lights). Using a thin piece of paper, the light-beam can be made visible. With the mirror placed on top of the mount, make sure enough light reaches the detector (place the paper in front of the detector window). If this is not the case, the sample screw must be turned. (typically not the case) When enough light reaches the detector, the experiment can be started.

During evaluation, the measured transmittance spectrum should be always corrected for reflectance. These results form the basis for ellipsometry measurements and its necessary simulations and should therefore be conducted with special care.

## 5.6. Infra-Red Spectroscopy (IR)

When talking about IR spectroscopy in thin-films of conducting polymers, scientists typically mean attenuated total reflectance- fourier transform infra-red spectroscopy (ATR-FTIR).[25,26] As a general introduction would be beyond the scope of this thesis, I will focus on caveats, troubleshooting and our equipment.

ATR-FTIR is a powerful technique for conducting polymers, as you can analyze an insoluble material in a non-destructive way with little material needed. Just as regular FTIR, you receive information about functional groups and hints towards adsorbed water, decomposition of your polymer, etc. Most importantly, the presence of infra-red-activated vibrations (IRAV- bands), is direct proof for the presence of a polymer. This is especially important when synthesis was done.

At LIOS, we have two instruments by the Bruker company, both useful, albeit for different materials.

The new engine (BRUKER VERTEX 80) can measure films deposited on most substrates- no special substrate is needed as a diamond is integrated into the measurement stage. This instrument measures a single reflection, thus a limited area and no special sample preparation is needed. As a consequence, this setup is ideal for quick measurements but is limited by the refractive index of the diamond. Also, it is not especially powerful due to a single reflection.

For some materials you will be therefore limited to the use of the old instrument (Bruker IFS 66/S). This is substantially more complex and its operation requires substantially more training and experience. As a reward, you measure multiple reflections (6) and thus get a stronger signal. Further, you can use ZnSe or Ge single-crystals, thus being able to measure materials of a higher refractive index, which proved crucial for PEDOT and PEDTT. This, however, means that you can only use a substrate that can withstand your synthesis conditions. Also, you might have to clean the edges of the substrate where the probing beam enters the single-crystal in order to perform a measurement.

In order to avoid signals from the substrate and also to get a signal similar to absorption, the signal should be presented in following way:

$$Abs. \approx -\frac{\Delta T}{T} = \frac{T_{polymer} - T_{substrate}}{T_{polymer}} \tag{1}$$

Results by any of the two engines present the basis for any further ellipsometry measurement.

## 5.7. Ellipsometry

Ellipsometry is a powerful technique that is typically used to measure thicknesses of well-known materials or vice versa the optical properties of a film with a known thickness. In this work, it was used to elucidate the optical parameters $\varepsilon_1$ and $\varepsilon_2$ of conductive polymers. In other words, the dielectric properties of the material were investigated optically, namely, the refractive index and dielectric function. Detailed information on this technique can be found elsewhere. [27,28]

The measurements for this technique were done at JKU, at the Center of Surface and Nanoanalytics (ZONA). They can offer devices measuring in the infra-red and UV-visible region.

All measurements will need to be modelled to receive meaningful data about your materials optical properties from the measured sample polarization. Therefore, good and precise thickness-measurement, IR, and UV-vis data present a great advantage for the interpretation of the measurement. Further, thin films (<100 nm) will limit interference effects; ideally two distinct thicknesses are investigated.

In case of the substrate, special attention has to be paid. First, an amorphous, transparent substrate should be used (glass), as a crystalline substrate would alter the results. In theory, it is only necessary if we exactly know the dielectric function (DF) of the substrate material. However, even small errors could cause artefacts if sharp resonances in the substrates DF are present.

Second, the substrates backside must be roughened thoroughly by sanding. For this, contact the workshop or our responsible technician. To avoid damage to the substrates front, attach scotch tape which will prevent any roughening of the measured surface. After sanding, remove the tape and remove any residues of glue by washing the substrates with acetone and deionized water. Consequently, you should have a substrate with one side shiny, the other side having a milky quality. Inhomogeneous or incomplete sanding will not be sufficient. Contrary to popular believe, the so-called "scotch-tape trick"[29], that is sticking a visually cloudy scotch tape to the substrates back-side instead of sanding it, was not sufficient for our measurements and caused serious complications during modelling. (back-reflection)

Special care is advised with respect to its cleanliness- the use of detergents (*i.e.* Hellmanex) should be avoided at all times as a layer forms, irreversibly attaching to the substrate which will interfere with your results.

As the measurement is done in air, the measured sample must be stable on air. This is especially true for measurements in the infra-red as a measurement might easily take several hours instead of minutes in the case of UV-vis.

Where the measurement is relatively straight forward, modelling of the results often presents a challenge. As mentioned above, transmission measurements are invaluable to this task. Another important information is thickness, which should be fixed during modelling. For laterally inhomogeneous samples, such as it was the case with PEDOT:sulphate, this can already be a challenge and the use of a concentrating lens to minimize spot size is recommended. The spot size is reduced then from 2x5 mm to 150x300 µm.

The weighted-mean of roughness can be simulated iteratively in the "CompleteEASE" software supplied by the ellipsometeres manufacturer, J.A. Woolam.

## 5.8. Profilometer

The Bruker Dektak XT presents an extremely powerful technique to measure sample thickness in a quick and efficient manner. For operation, contact the master user in order to receive proper training.

Three things should be, however, kept in mind.

First, use a clean, unbent needle with a straight tip and gently scratch the surface. You will not need force to do so- excessive force will just render the needle useless for further use.

Second, perform multiple measurements, ideally as close the relevant area, for instance next to where you measure conductivity or absorption. As this technique is destructive, this should be performed after measurement, if possible.

Third, extremely rough samples might prove challenging and might require estimation from your side to get an average thickness. This is necessary, yet might cause problems in ellipsometry measurements.

## 5.9. Specialized Techniques for collaboration

In this section, I will focus on good collaboration practice and important details to keep in mind when collaborating with other researchers and master users of specialized techniques. The simple reason is that detailed understanding of these techniques is not essential and can be learned from a textbook, while caveats are usually omitted.

In order to obtain information about you conducting polymers crystallinity and thus degree of structural disorder, x-ray diffraction[30] (XRD) is the technique to go to. Each engine has its own source of x-rays and thus might or might not be suited for your material. The same is true for x-ray reflection[31]. (XRR) XRR can helps to elucidate the total electron density (per volume) and also sample-roughness. Make sure to supply your operator is supplied with sufficient literature and make sure both sides understand the aim of the measurement. Also, organic materials are in many ways complex and hard to measure and it pays-off to contact a specialist. Collaborations in this regard are well established with our institute.

1D XRD of a crystalline material will result in a number of peaks, some of them caused by the substrate, which is why a blank measurement is of essence. The broader the peak, the smaller the crystals and thus the more disorder. This relation is relied upon when the Scherrer formula[30] (formula 1) is used to estimate the crystal size from the peaks full-width at half-maximum (FWHM).

$$\tau = \frac{0.9 \cdot \lambda}{\beta \cdot \cos\theta} \qquad (2)$$

where τ is the minimum crystallite size, λ is the wavelength of the incident radiation, β the FWHM of a selected Bragg peak, and θ is one-half of the scattering angle 2θ. The prefactor 0.9 is chosen assuming spherical particles- other forms of particle require a different pre-factor, typically on the order of unity (in the range 0.80-1.05). Unless corrections are applied, the result represents the minimum crystallite size observed.

Keep in mind that a certain a peak and thus structural order might be induced by the underlying substrate and thus a separate measurement on a different substrate might be of interest.

The presence of peaks indicates local ordering- how well these features are connected among each other is not known, meaning that sufficient electronic disorder i.e. scattering on the grain boundaries might still impede electron transport, hence quenching conductive properties.

X-ray photoelectron spectroscopy (XPS), or electron spectroscopy for chemical analysis (ESCA) is another specialized technique that can deliver crucial information about your conducting polymer. It is a highly surface sensitive technique (>10 nm), which enables us to identify the elemental and also chemical composition of the surface.

The surface is irradiated with X-rays (*i.e.* $AlK_\alpha$ = 1486.7 eV), which leads to emission of photoelectrons of kinetic energy, $E_{kin}$. Based on the excitation energy, $h\nu$, and the instruments workfunction, $\varphi$, the binding energy of these electrons, $E_B$, can be derived by:

$$E_B = h\nu - E_{kin} - \varphi \qquad\qquad (3)$$

In insulating samples, the emission of photoelectrons can lead to surface charging, which can be compensated by using a dual flood gun, providing both $Ar^+$ ions and electrons. This might, however, lead to the degradation of the sample.[32]

The binding energies are typically referenced by either observing the $Au4f_{7/2}$ (84.0 eV) peak or by assigning the C-C/C-H contribution at 285.0 eV. As for that purpose carbon is sometimes added, instruments may show carbon pollution in the form of so-called "adventitious carbon", setting-off the actually measured carbon concentration.

Following information can be gained: First, elemental composition and potential elemental impurities can be determined. Therefore, in thin samples with bad substrate coverage the substrate material will be observed as an additional peak (*i.e.* an inhomogeneously covered gold substrate will show a gold-peak).

Second, based on the expected chemical composition and available literature, the molecular composition can be estimated. The oxidation state of an element will result in a shift in the peak, making resolution of functional groups possible. By fitting the measurement results by individual peak-shapes and integration of these, the chemical character of the surface can be analyzed. Comparing the integrals, chemical identity and the ratio of monomer to counter-ion can be estimated.[33,34]

For organic, conductive polymers, we need to worry about chemical stability during measurements and therefore carefully choose the measurement conditions to avoid concentration gradients during measurement. Also, it should be kept in mind, that because XPS is a highly sensitive surface-technique, we might not get the true ratio's present in the bulk.

A good help during result evaluation can be found here: https://xpssimplified.com/elements/

Another useful technique in the context of CP's is MALDI-MS. It is a destructive analytical technique requiring several *mg* of material. On the other hand it will directly prove if the monomer was stable and if so, can deliver polymerization lengths being present in the material. This in itself present a crucial contribution and makes the possibly large effort worthwhile. All measurements in the context of MALDI-MS were conducted at the Institute for Chemical Technology of Organic Materials.

Transmission electron microscopy (TEM) presents another electron-irradiation based technique. For this technique, however, a conductive polymer film must be placed on top of a copper-grid instead of being measured directly on top of the substrate it was deposited on. The big advantage of this technique is that you simultaneously record a real-space image of the polymers features, but likewise observe its electron scattering pattern (reciprocal space). In the case of a crystalline sample, not only its real-space shape can be observed, but also a symmetrical diffraction pattern will show, facilitating any argument concerning local structural order. As such, it is complementary to any XRD measurement.

## 6. Theory

### 6.1. Disorder

Disorder is deemed one of only two factors[12] resulting in the conductive properties of a conductive polymer. The other important factor is found in the chemical composition of the material, i.e. the polymer relied upon as well as the counter ion used.

Disorder theories originate from studies of inorganic materials, however, many of the concepts being valid for organics as well. [6,11,35–40]

Typically, disorder theory of inorganic conductors was mainly limited on general disorder, that is structural and chemical imperfections resulting in altered conductive properties, i.e. electronic disorder. As organic conductors are typically molecules arranged in hierarchical, structural order, the situation is slightly different:

1. Intra-molecular conduction plays a role in conductivity of organic molecules.

2. Organic molecules are arranged in ensembles with their relevant doping agents and impurities. Their interaction causes alteration of the energy of available states which can be occupied by electrons.

3.In case of the formation of crystallites, a special case of point 2, the electron transport across the grain boundaries and hence a minimal carrier scattering across these becomes crucial.

In short: The word disorder describes a number of complex, possibly interconnected parameters impeding on the transport of charge carriers through the system and is thus an ensemble of parameters summarized by one. Thus, a number of strategies for its minimisation is applicable. Strategies include:

1. Creation of an energetically flat intra-molecular charge-carrier transport profile by a flat, planar, conjugated system.[41–43] For this, the main representative is found in PEDOT.

2. Slow polymerization processes to maximize chain-length and the overlap between these as well as avoidance of introduction of impurities.[44]

### 6.2. Conductivity in Disordered Systems

Conductivity in structurally ordered systems such as crystalline metals or conventional, crystalline semiconductors (*i.e.* silicon) is typically described by band transport. In non-crystalline materials, i.e. disordered metals[45], a different form of conduction is present. Instead of the typical, positive temperature coefficient of resistivity (TCR) at elevated temperatures with a saturation when vibrations reach their energetic minimum, an increase of conductivity upon heating is expected. A material of low disorder, on the contrary would be expected to show a temperature independent or even metal-like conductivity profile. This can be imagined as a result of full delocalization of carriers.

In order to explain the observed conduction mechanisms, the so-called hopping mechanism was proposed, often referred to as variable range hopping (VRH).[46–48] This conduction method describes a temperature activated type of transport of localized charge-carriers "hopping" to unoccupied energy levels within a solid. The energy difference between states and their relative distance determines the hopping probability at a given temperature.

This describes transport of carriers between a number of localized, empty states. The energy to transverse from one state to another is gained by thermal activation. Consequently, at low temperatures, conductivity tends towards zero.

In conducting polymers, the term of weak localization is often used, describing a limbo-like state where localization is yet hampering the conductivity, still metal-like properties begin to appear

such as a finite conductivity at low temperatures, a flat temperature profile of conductivity, and in the rare case of metallic conducting polymers, the appearance of positive MC or the metal-insulation transition (MIT).[3–5,7,8,10,49]

The most convenient way of characterizing a materials position relative to the MIT is the construction of the Zabrodskii[50] or W-plot. In this, resistivity (or conductivity) is reformulated as the parameter W, which corresponds to following:

$$W = - \left[ \frac{\partial \, ln\rho}{\partial \ln T} \right] \qquad (4)$$

which if calculated from conductivity changes to

$$W = \left[ \frac{\partial \ln \sigma}{\partial \ln T} \right] \qquad (5)$$

where $\rho$ is the resistivity, T the temperature in Kelvin and $\sigma$ the conductivity.

It should be noted, that W is representative of the reduced conduction activation energy.[51]

$$W = \frac{\varepsilon}{kT} \qquad (6)$$

where $\varepsilon$ is the activation energy of transport and kT is equivalent to the thermally available energy. (Arrhenius type charge transport)

This parameter W has to be plotted in a double-log plot (for better visualization), resulting in three possible trends:

**1. a negative slope**

This is typical for materials subject to temperature activated electron transport. As a consequence, materials exhibiting such a kind of behaviour are termed to be in the insulating regime.

**2. a flat contour**

A flat contour means the conductivity is subject to the so-called power law or temperature independent transport. In general, the materials is described to be in the critical regime of the MIT.

**3. a positive slope**

Such a slope is a hallmarks of metallic transport. The material is described as a glassy metal.

Another consequence of plotting your data in a double-log plot, is the loss of representation of any negative values. As a consequence, the W plot of a metal such as silver would result in a blank graph as a positive TCR would mean a W-value <0. In this case, we talk of a crystalline metal.

The conductive properties of a material while applying a magnetic field can be significantly different from a field free measurement. As a general rule, a strong magnetic field typically worsens a materials conducting properties which is typically explained by boosting electron-electron interactions rather than weak localization.

## 6.3. Magnetoconductivity

Measurement of conductive properties while applying a magnetic field was described above and is typically not referred to as magnetoconductivity (MC). In order to monitor the sole effects of a magnetic field on conductivity, the magnetic field is ramped at low, fixed temperatures.

A set of explanations for the necessity of low temperatures is given by Kaiser and Skákalová[47,52]. First, they point towards weak localization. Typical for disordered conductors, a change in scattering type occurs during cooling a conducting system: At high temperatures, inelastic scattering prevails, i.e. charge carriers can easily interact with phonons, causing their emission or absorption. At low temperatures where phonons are at their energetically lowest state, elastic scattering dominates. Consequently, in case of backscattering, charge carriers keep their relative phase, leading to a constructive interference and a diminishing of conductivity. A magnetic field can then change their relative phase, thus counteracting said decline. Consequently, MC measurements are the method of choice to determine the presence of weak localization.[47]

Second, electron-electron interactions are mentioned as a reason for the necessity of low temperatures. Imagining a situation similar to variable range hopping (VRH), where electrons can be conducted only by occupying a discrete state, band splitting would improve the possibility of an empty state being available in the right spin (positive MC). Shrinking of the available orbitals and thus hampering of the transition between states would result in a decrease in conductivity (negative MC, magnetolocalization, ML).

The reason for the necessity of low temperatures in the case of electron-electron interactions can be seen according to following relations:

The magnetic field splits the energetic levels of electrons, leading to an energy difference as follows:

$$\Delta E = m_s g_e \mu_B B \tag{7}$$

where $m_s$ is the electrons magnetic moment (±1/2), $g_e$ the Landé g-factor (2.0023), $\mu_B$ is the Bohr magneton (=5.79x10$^{-5}$ eV/T) and B the magnetic field in Tesla.

On the other hand, the thermal activation energy of a system corresponds to:

$$E = kT \tag{8}$$

where k is the Boltzmann constant (= 8.62x10$^{-5}$ J/K) and T the temperature in Kelvin.

The larger the thermal energy of the system with respect to the band-splitting energy supplied by the magnetic field, the less expressed the contribution of the magnetic field on the conductivity is expected.

Equating both sides of the equation, we can relate the thermal energy to energy difference of the now split energy bands. We expect the influence of a magnetic field to be observable when both energies are in the same range. The results of this calculation can be found in table n below.

| B / T | T / K |
|-------|-------|
| 1 | 0.7 |
| 3 | 2 |
| 6 | 4 |
| 9 | 6 |

Table 8: Magnetic field and temperature related in terms of available energy

It should be kept in mind, that equation (7) is typically applied for localized, unpaired spins in Electron Spin Resonance spectroscopy and does not consider the much more complex situation of delocalized/weakly localized electrons.

In order to visualize the results of a MC measurement and make the changes comparable between different temperatures, the conductivity changes are plotted relative to the B-field, as follows:

$$\frac{\sigma - \sigma_0}{\sigma_0} = \frac{\Delta\sigma}{\sigma_0} \quad\quad\quad (9)$$

where $\sigma$ is the conductivity at a given magnetic field and $\sigma_0$ the conductivity without a magnetic field applied. (to show the change in percent, multiply by 100)

In most conductive polymers, the plot will result in negative values as electron-electron interactions are enhanced, thus decreasing the materials conductivity. This phenomenon is referred to as magnetolocalization or negative MC.

In some rare cases[3,4,6], an interplay of positive and negative MC was observed. At low magnetic fields, the effects of weak localization and electron-bandsplitting prevail. This effect is referred to as positive MC as it results in an increase in conductivity. Eventually, magnetolocalization will prevail, hampering charge carrier conduction and thus resulting in negative conductivity. These effects are described by the formula given below:[53]

$$\Delta\sigma = +0.041\alpha \left(\frac{g\mu_B}{k_B}\right)^2 \gamma F_\sigma\, T^{-3/2}\, H^2 + \left(\frac{1}{12}\pi^2\right)\left(\frac{e}{c\hbar}\right)^2 G_0 (l_{in})^3 H^2 \quad\quad (10)$$

where $\alpha$ and $\gamma F_\sigma$ are parameters, $G_0$ is $\left(\frac{e^2}{\hbar}\right)$, and $l_{in}$ is the inelastic scattering length.

At low temperatures, the first part is proportional to $H^2$ whereas the latter is proportional to $H^{1/2}$.

The results of MC measurements can be further used to estimate the scattering length or mean free path of charge carriers by reformulating the magnetic field as the Landau orbit size, $L_D$,[54–57]

$$L_D = \sqrt{\frac{\hbar}{e\vec{B}}} \quad\quad\quad (11)$$

where $\hbar$ is the reduced Planck constant, e the elementary charge and B the magnetic field in Tesla.

The conductivity maximum in the MC measurement represents a resonance event caused by the magnetic field, where carriers experience maximum delocalization- in the sense of the Landau orbit size they observe the mean free path of carriers, $\lambda_e$.

$$L_D = \lambda_e \quad\quad\quad (12)$$

Note, that other more direct, but also more specialized techniques for the estimation of mean free path are available, also.

## 6.4. Hall effect - general case

The Hall effect describes a phenomenon in solid state physics, where charge carriers moving through a solid are deflected by a magnetic field, based on the Lorentzian force. The direction of deflection is dependent on a carriers charge, allowing for the determination whether the majority charge carriers are either electrons or holes. Besides that, other parameters such as carrier mobility and carrier concentration can be determined by this technique. These two examples,

especially their determination by a single experiment, represent probably the biggest advantage of this technique.

The experimental setup typically involves at least four contacts, two of which are used to deliver a current, the other pair, situated perpendicular to the current flow to measure a voltage change. Perpendicular to the plane of conduction, that is perpendicular to the cross formed by the contacts, a magnetic field is applied. Depending on strength and sign of the field, B, carriers are deflected to either one or the other side, depending on their intrinsic charge, resulting in a measurable voltage, the Hall-voltage, $R_H$. Consequently, the Hall voltage plotted against the magnetic field, B, should result in a monotonous, slope: in the case of electrons of negative, in the case of holes of positive pitch.

As mentioned above, the minimal number of contacts is four, but this would require machining of evaporation masks to the most minimal of tolerances. The reason for that lies in the misalignment voltage, an offset in measured voltage due to imperfections in the alignment of the voltage leads. A possible way how to minimize these effects is the introduction of multiple voltage contacts and averaging their relative voltage-readings. (i.e. a Hall-bar)

## 6.5.  Hall effect - disordered systems

Hall measurements in disordered systems pose a significant problem as compared to measurements in crystalline materials. Disorder can manifest in various ways, including macroscopic sample in homogeneity, the charge carriers being preferably conducted in way generating a default offset current.

In order to measure a Hall effect in disordered materials, the carrier density must be large and disorder low, i.e. only low resistance, high mobility samples are expected to show any effect.[58] Further, well defined contacts are key to success. (ideally lithographically prepared or at least evaporated using a lithographically prepared shadow mask) Still, ultimately only a hand-full of organic, disordered materials were reported to show a Hall-effect.[59,52,60]

From the measurement data, it is possible to extract information about the materials charge-carrier transport properties such as mobility and charge carrier concentration. In this context, Kubo's work should be mentioned, presenting an alternative to classical drift formulas to describe mobility in the presence of disorder (by a statistical-mechanical theorem) On this work, Friedman based his Random Phase Model (RPM) that allows interpretation of the Hall effect data in non-crystalline solids. Therein, Hall- and drift-mobility are related by a number of factors:

$$\frac{\mu_{Hall}}{\mu_{Drift}} = \frac{6\,k_B T}{J}\left(\eta \cdot \frac{\bar{z}}{z^2}\right) \tag{13}$$

where J is a factor related to the bandwidth, z the atomic coordination number, $\bar{z}$ the average coordination number, and η the parameter derived from the Hall angle.

The bandwidth and J are related by following formalism:

$$\Delta(E_C - E_F) = W_B = 2zJ \tag{14}$$

From the conductivity-temperature dependence in the hopping regime (temperature activated transport) we estimate $W_B$.

$$ln\frac{\sigma_{T\ activated}}{\sigma_{300\,K}} = ln\frac{\Delta(E_C - E_F)}{k_B T} \tag{15}$$

Friedman states following guideline for the other parameters:

$$z = \bar{z} = 6 \tag{16}$$

and

$$\eta = \overline{\cos^2\theta_H} = \frac{1}{3} \tag{17}$$

Relating the activation energy to 1 meV or 11.3 K, we arrive at

$$\mu_{Hall} = \frac{4k_BT}{W_B} \cdot \mu_{Drift} \tag{18}$$

with T being the sole variable between Hall and drift mobility.

In order to gain the Hall mobility, $\mu_{Hall}$, we return to the measurement data, *i.e.* the Hall voltage: we calculate the Hall coefficient, $R_H$.

$$U_{Hall} = R_H \frac{I_{xx}B}{d} \tag{19}$$

where $R_H$ is the Hall constant, $I_{xx}$ the current, and d is the thickness of the conductor.

From the Hall-constant, we can calculate the number of carriers thanks to

$$R_H = (en)^{-1} \tag{20}$$

and consequently the Hall mobility, $\mu_{Hall}$, from the conductivity:

$$\sigma = en\mu_{Hall} \tag{21}$$

or

$$\mu_{Hall} = \frac{\sigma}{R_H} \tag{22}$$

Relating now to formula 15, we arrive at the drift velocity.

The carrier density can be further normalized per monomer subunit if the material density is known:

$$\frac{\rho}{M} \cdot N_A = N_{Monomers} \tag{23}$$

where M is the molar mass of the monomer (including the doping ion- therefore the doping ratio must be known, *i.e.* from XPS).

Consequently:

$$100 \cdot \frac{n}{N_{Monomers}} = \% \, doping \tag{24}$$

## 6.6. Pressurizing organic conductors

Applying pressure to a material can have severe effects to said materials conductive properties. Pressure can both, positive and negative effects.[53,61–63] Organic conductors, however, typically respond well to applied pressures.[53,63,64]

On the contrary to popular opinion, simulations have shown relatively small pressures are needed to compress molecules in van-der-Waals (vdW) crystals.[65,66] A comprehensive study on pressure-effects on disorder in polythiophenes can be found here.[67]

Typically, a pressurization medium needs to be used in order to deliver the pressure to the sample without destroying it permanently. An example is the Daphne 7373.[68]

## 6.7. Considerations for Synthesis of Metallic Polymers

The rationale developed for the synthesis lies in simplicity and minimization of human error. As previously mentioned, CVD was relied upon to deposit conductive polythiophenes.

The choice of monomer becomes crucial.

First, we need to minimize disorder. Therefore, the ideal monomer should have only two, symmetric reactive sites. Thiophene has 4 reactive sites of various reactivities. Consequently there is a non-zero probability of branching. In poly(3-hexyl thiophene) (P3HT), one reaction site is blocked, reducing the 4-positions reactivity. Despite that and tremendous optimization efforts, the conductivity record in this polymer is found at 12.7 S/cm, only.[69] Consequently, both positions, 3 and 4, should be protected, just as it is the case in PEDOT, which sports state-of-the-art conductivities in the thousands of Siemens.[7–9]

Further, polymerization should readily occur. This has to be found empirically and should fit the polymerization reaction you intend to apply. The method employed in this thesis was shown to work for multiple polythiophenes, but becomes more challenging for non-thiophene systems. Hence, I will focus my consideration on thiophenes and thus the substitution of the 3,4 positions, only.

In order to increase the reactivity of the 2 and 5 position, both should be electron rich. Substitution by electron pushing atoms is advantageous, yet it is crucial to consider both mesomeric (*i.e.* by free electron pairs) and inductive effects (by electronegativity/electron deficiency). Oxygen in the form of an ether-bond, for instance, is a viable choice while fluorine will definitely be counter-productive. In general, functional groups should be as compact as possible and should influence factors such as polarity or acidity as little as possible in order to achieve high conductivities. This is different from functional polymers, *i.e.* used for $CO_2$ reduction.

Further, it is not only important to have a compact, simple polymer, but it also needs to be flat. A flat structure will always beat a polymer with a large dihedral angle as this effectively breaks conjugation and inhibits delocalization. Consequently, it is advantageous to introduce functional groups that interact with each other such as hydrogen-bonds, ionic attractions or non-covalent sulfur-oxygen bridges.[42]

At last, I would like to point out that most studies neglect the importance of the counter-ion. We employed sulphate (or a hydrated form of it) to be our counterion. It is relatively small, its disruptive effect on the matrix is therefore minimal. Further, sulphate-salts readily form large crystals. At last, the consideration of S-O bridges might improve integration of sulphate-ions into the polymer matrix.

Many of the herein presented principles can be found in the reviews by Roncali [41,43] or theoretical work from others.[70]

Based on these considerations, Figure 5 shows the possible advantages and properties of the monomers used in this thesis. All three monomers are structural analogues, yet despite that, different electrical properties are expected.

First, PEDOT combines all the advantages described above. A dense packing and flat polymer chains favour delocalization.

Second, PEDTT should exhibit similar properties, except for planarity. The ring-substitution is relatively stable, the electron density is possibly slightly increased as we "go down" the periodic table of elements. On the up-side, a strong interaction with sulphate is expected due to multiple S-O bridge that can form. Consequently, the counter-ion might work as a structurally stabilizing influence.

Third, we have PTP. The use of nitrogen atoms requires three C-N bonds to be formed to avoid the availability of a proton on the monomer. As we intended to observe structural analogies, we arrived at two additional reactive sites and a source of additional disorder needs to be expected. Further, sulphate does have only one sulphur per monomer to form bonds to. The stability of doping is thus of the question. Therefore, amongst the three materials, the worst conductivities are expected in PTP.
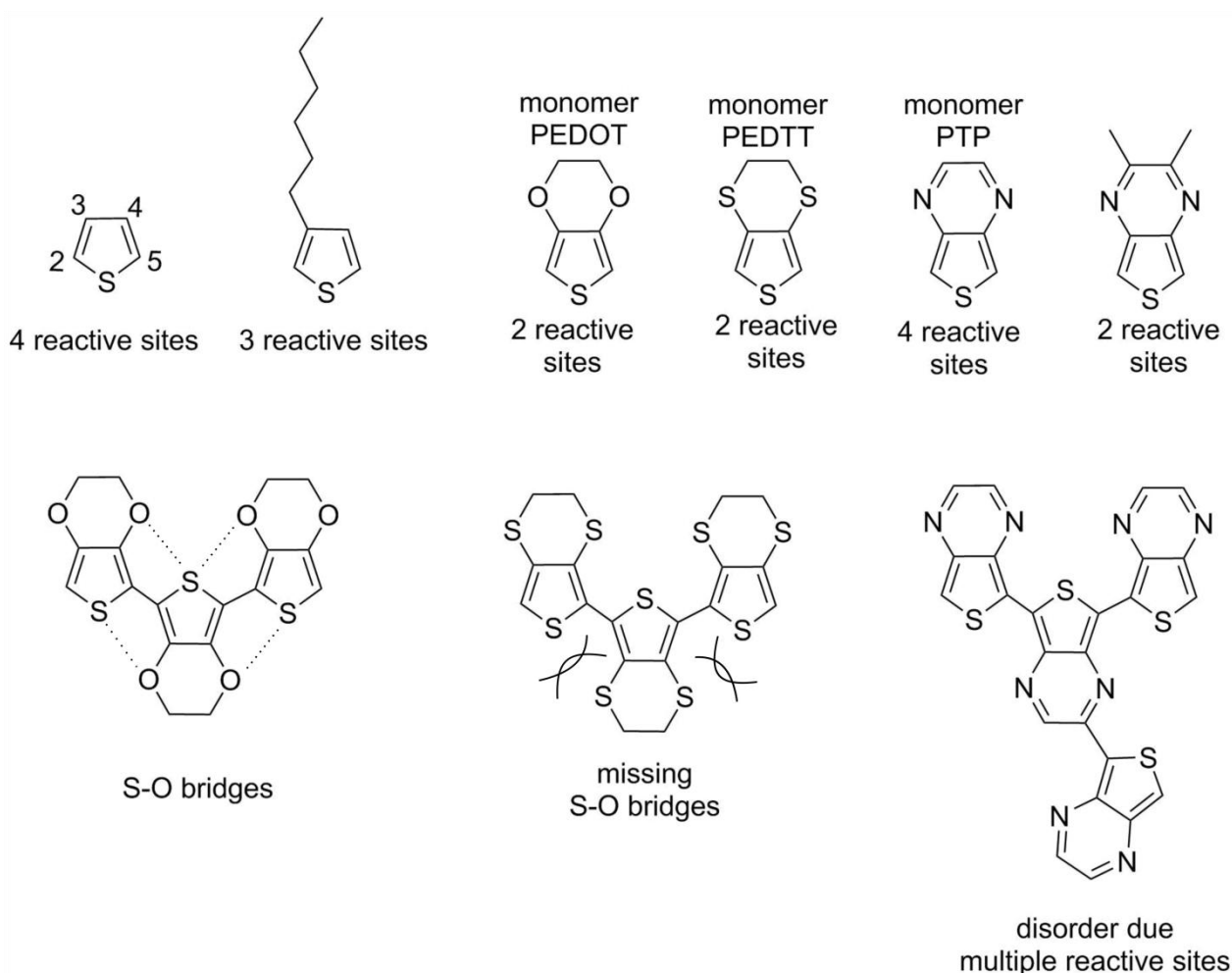


Figure 5: Various thiophenes with their peculiarities pointed out with respect to polymerization. The principles described above are illustrated by the thiophene derivatives shown in this Figure for graphical representation.

# 7. Results and Discussion

## 7.1. PEDOT: sulphate thin films

PEDOT:sulphate presents the conceptual flagship of this thesis. The material is renowned for great electrical properties and sufficient literature has accumulated since its establishment in order to conduct improvements based on rational rather than serendipity.

Films were grown as described in the experimental section.

The films would delaminate in the presence of water or alcohols unless grown on top of a self-assembled monolayer (SAM) of ortho-octyltrichlorosilane (OTS). It could be easily removed off of glass or sapphire by scotch-tape.

Parts of the herein presented data were previously published elsewhere by the author.[6,71]

### 7.1.1. Charge carrier transport

By fully focusing on the suppression of disorder, it was possible to obtain a significant achievement in terms of conductivity. At room temperature, 4050 S/cm were reached with minor losses when cooling down to low temperatures such as 1.8 K. At that temperature, about 3300 S/cm or 81% of the original value remained, a record in itself. The initial increase in conductivity upon cooling can be interpreted as an interplay between thermal activation and mechanical contraction of the sample facilitating inter-molecular transport.(Figure 6a) At low temperatures, a flat contour can be observed, typical for metallic polymers, indicating temperature independent transport. (Figure 6b)

MC measurements are often relied upon when observing conductive polymers. If weak-localization is dominant, an interplay between MC and ML should be observable. Consequently, conductivity measurements were repeated at low temperatures in the presence of a magnetic field (Figure 6c,d). Magnetic fields of 0-9 T were applied on a sample cooled to 1.85-10 K, respectively. ML was the strongest at 9 T, and an indirect dependence on temperature could be determined. The strongest dependence was found at -5% with respect to the absence of a B-field. At fields below 4 T, MC was the dominant observable at all investigated temperatures. This indicates that we have a transition between weak-localization being the dominant influence at low fields, whereas electron-electron interactions become dominant at high fields. (Figure 6d)

In the case that an interplay between MC and ML can be observed, it is possible to estimate the charge carriers scattering length or mean free path from the Landau orbit size. For this, the magnetic field needs to be reformulated (see theoretical part). At the maximum, *i.e.* at the resonance, the mean free path is found. (Figure 6e) At the lowest temperature, the mean free path was found to be the largest with more than 33 nm, whereas at 10 K it would have recessed to 15 K. This indicates a large degree of delocalization beyond the scale of a single PEDOT chain.

Another way of presenting conductivity data is the W-plot (for further information see theoretical part). In this plot, an upward-pointing slope indicates a metallic system as found in a disordered or "glassy" metal. (Figure 6f) The black line shows the conductivity-measurement at the absence of a magnetic field, which clearly shows a metallic behaviour at low temperatures. At a B-field of 9 T, the slope turns flat at first, indicating the material to be in the critical regime of the MIT. Below 4 K, however, the system reverts back to a metallic regime. This means that even a strong magnetic field cannot fully suppress the materials metallic properties.
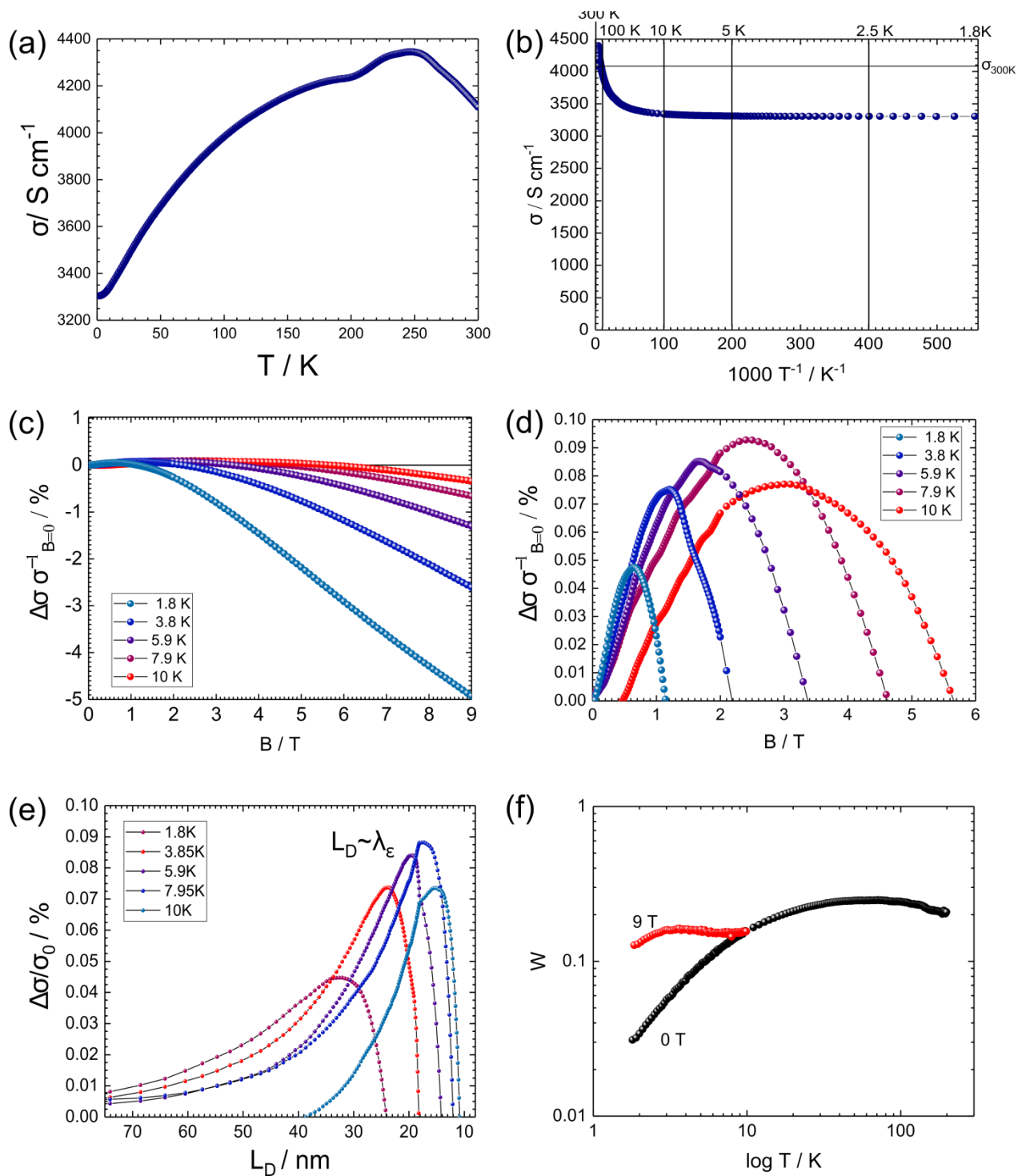
Figure 6: Charge transport properties of PEDOT:sulphate thin-films.[6] (a) Conductivity profile. (b) Reciprocal temperature profile.(c) Magnetoconductivity measurement. (d) Zoom on positive part of (c). An interplay of magnetoconductivity (MC) and magnetolocalization (ML) can be observed, indicating metallic properties. (e) Reformulation of MC-data into Landau orbit size. (f) W-plot with and without a magnetic field. In the absence of a B-field, properties of a glassy metal are observed that will only be partially quenched by a strong magnetic field of 9 T.

### 7.1.2. Chemical identity

A typical argument we encountered during our work on PEDOT:sulphate was if the monomer would survive synthesis or be degraded in some way. Therefore, XPS was consulted. Further, the degree of polymerization (*i.e.* chain-length) was investigated by MALDI-MS.
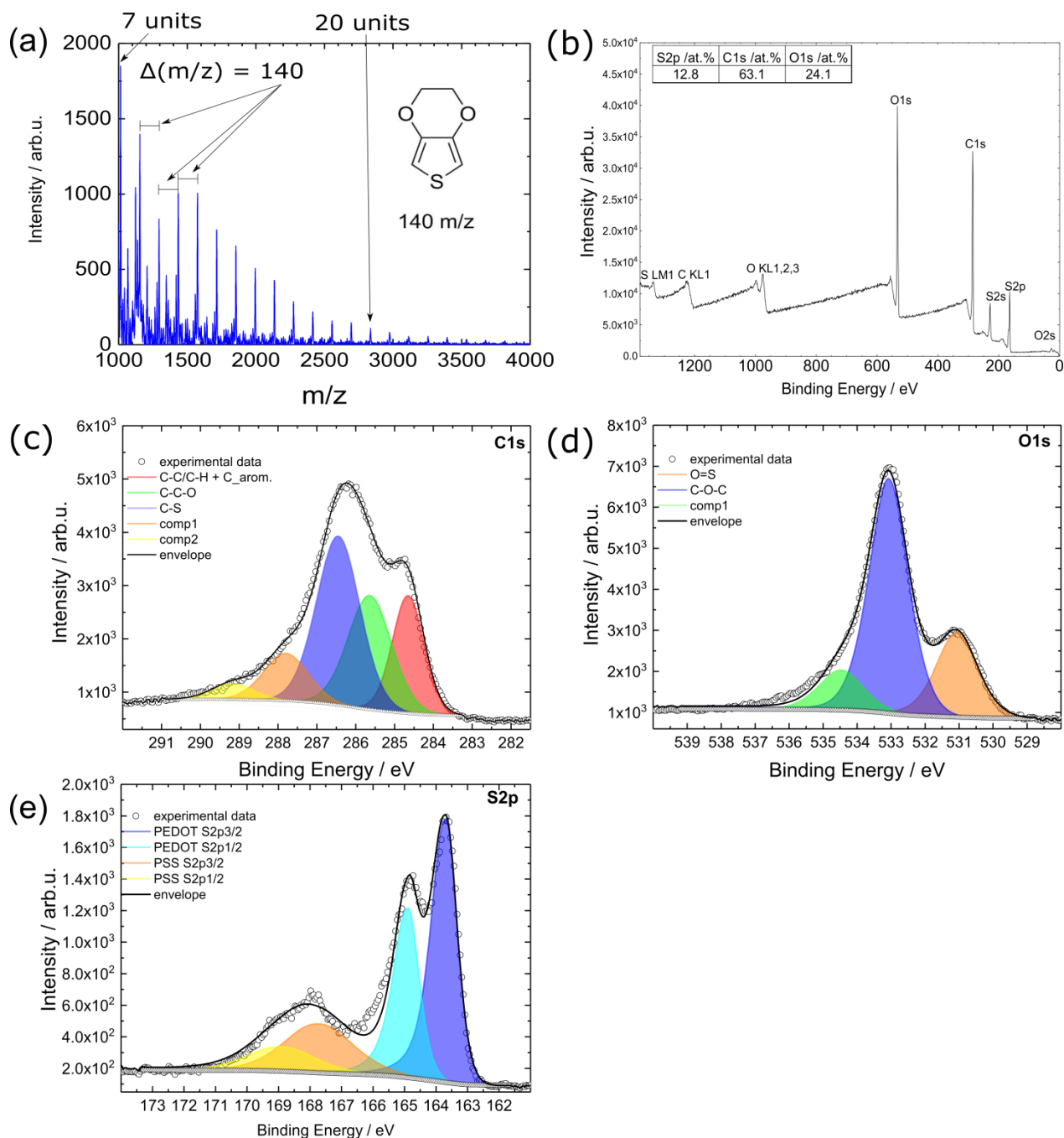


Figure 7: Chemical characterization of PEDOT:sulphate.[6] (a) MALDI-MS revealing chain-lengths between 7 to more than 20 units. (b) XPS survey revealing O, C, and S in amounts of 12.8, 63.1, and 24.1 at%, respectively. (c) C1s spectrum. The components match the expected stochiometry. Comp1 and comp2 possibly adventitious carbon. (d) O1s spectrum. Additionally to the expected signals, an unknown component was found, probably related to the adventitious signal found in the carbon high resolution scan. (e) S2p spectrum revealing PEDOT and sulphate contributions.

In order to determine polymer chain-length, MALDI:MS was conducted. (Figure 7a) Thanks to unchanging, stable monomers, it was possible to determine the presence of a pattern. The spectrum was measured between 1000-10000 m/z ratio. A stable spacing of 140 was found, corresponding to the molar mass of PEDOT lacking 2 hydrogen atoms which are lost during the

reaction. The biggest fraction was found to be the heptamer of PEDOT, but even eikosomers (20 repeat-units) and larger were found.

A survey scan revealed an elemental purity in the material, revealing the presence of oxygen, carbon, and sulphur. (Figure 7b) The oxygen, sulphur, carbon ration was determined to be 12.8: 63.1:24.1, respectively. The absence of gold indicates uniform, pinhole-free coverage. The presence of hydrogen cannot be determined from XPS but can be assumed from basic chemical principles. Detailed scans of the elements revealed by the survey were attempted. The results were compared with literature on PEDOT:polystyrene sulfonate (PSS).[72,73]

Carbon C1s high resolution scans revealed C-S, C-O, and C-C/C-H bonds being present in the polymer matrix, as well as adventitious carbon. (Figure 7c) Contrary to literature, the main contribution was from C-S and not from C-C/C-H, which is to be expected as no PSS is was added. This is indicates that PEDOT makes up the bulk of the material and any organic contaminations are present in traces at worst. The ratio of the peak-integrals indicate that the measured material truly is PEDOT.

Oxygen O1s scans revealed O-S, and C-O-C bonds present in the films. (Figure 7d) The sulphur contribution was substantially lower which supports our hypothesis, that simultaneous doping and deposition would lead to an ideal ratio of both components.

Sulphur S2p scans revealed peaks typical for S-C and S-O bonds. (Figure 7e) The oxygen and sulphur scans support each other in the sense that a lower dopant-concentration than in commercial PEDOT:PSS. The monomer-to-dopant ratio was determined to be 2.8 monomers per sulphate ion.

### 7.1.3. Structural properties

When the chemical identity was confirmed, the data was partially explaining the extraordinary conductive properties. However, structural data from XRD and TEM represent the only way of probing structural disorder. Structural properties of PEDOT were investigated mainly in two ways: x-ray- and electron-based techniques.[71]

For x-ray based techniques, XRR[31] was relied upon to give information on roughness and electron density. (Figure 8a) The angle of total external reflection ($\alpha_c$) was observed at 0.195 °. This corresponds to an electron density of 543 nm$^{-3}$. Above said angle, the intensity of the peak decreased dramatically, which together with the missing of Kiessing fringes suggests a relatively rough sample.

Further, XRD was conducted (Figure 8b) to investigate the crystal structure, revealing 3 distinct peaks: 6.59, 19.80, and 23.74°, corresponding to a spacing of 1.341, 0.448, and 0.375 nm, respectively. The presence of only three peaks suggests a preferred orientation relative to the substrate, possible edge-on and face-on. The first and third peak seem to belong to the same series, *i.e.* 001 and 003 or the first and third-order reflection of the same series.

Combined with the results from XRR it lead to the impression of an archipelago-like structure, where islands of large, structurally uniform and ordered features are separated by a sea of amorphous material.

This revealed a possible stacking geometry as indicated above. (Figure 8c) As we see it, the sulphate ions are intercalated between three PEDOT chains, neatly filling out the gaps and coordinating to the sulphur-atoms of the thiophene ring and the hydrogen-atoms of the third chain. The stacking distance was determined to be 0.375 nm and the separation in z-direction 1.36 nm, neatly fitting our projection.

At last, TEM experiments were measured. (Figure 8d-f) The archipelago theory was widely supported by the results shown herein. Crystallites were found to be in the range of 50 nm which is in good agreement with XRD results. The single crystal and the electron diffraction pattern shown, correspond to each other. (Figure 8e,f) The strong pattern that can be seen supports the XRD conclusion, that a high degree of structural order is present in these crystals.
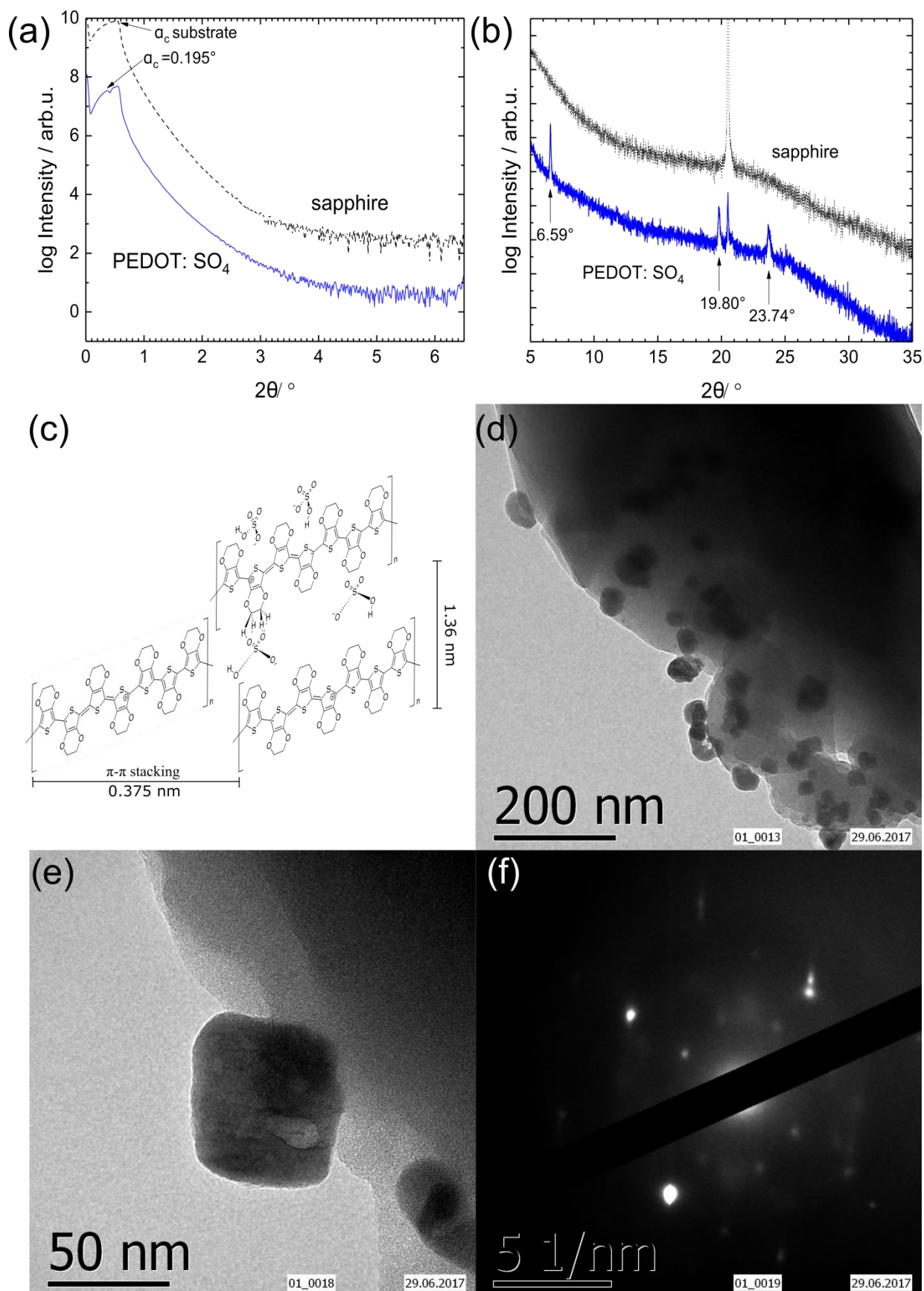
Figure 8: Structural data of PEDOT:sulphate.[71] (a) XRR data relative to sapphire. A rough sample with a total electron density of 543 nm$^{-3}$ was observed. (b) XRD data relative to sapphire. 3 distinct peaks were obtained. The Scherrer formula indicates structures of 80 nm. (c) Edge-on orientation of polymer with integrated sulphate ion. Three chains parallel to each other form a "triangle" with the sulphate intercalated in between the chains. The doping ratio from XPS data was assumed. (d) TEM measurements of PEDOT on copper grid. Black structures are PEDOT:sulphate single crystals. (e) Electron diffraction pattern.(f) TEM-detail of single crystal of ca. 50 nm in diameter.

### 7.1.4. Hall Effect

With high enough conductivity and strong indications for metallic properties, it was attempted to measure the Hall effect.
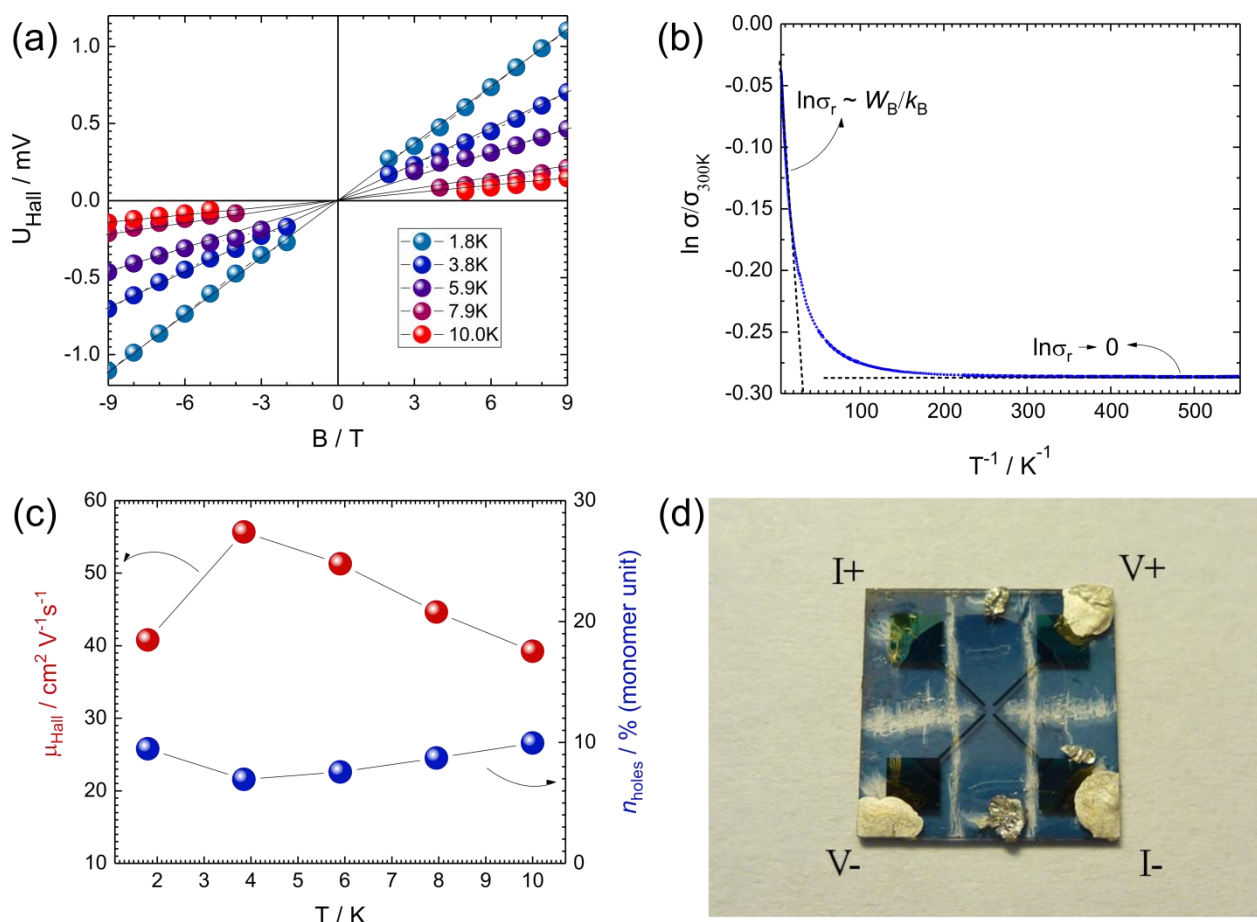


Figure 9: PEDOT:sulphate Hall effect data.[6] (a) Hall effect with positive and negative B-field applied. (b) Arrhenius type and metallic transport derivation plotted in order to derive the bandwidth, $W_B$. (c) Carrier concentration and mobility of carriers at different temperatures derived from the Hall measurement. (d) Sample for Hall measurement with denoted contacts.

Measuring at temperatures below 10 K, the magnetic field was ramped in positive and negative direction, leading to a linear response. (Figure 9a) At higher temperatures higher fields were necessary to obtain a linear response. Note, that the majority charge carriers were determined to be holes, as expected. (positive sign)

In order to deduce more information such as charge carrier density and drift mobility, the formalisms by Friedman were relied upon. (see theoretical part) The bandwidth was deduced from plotting conductivity data as the natural logarithm of the conductivity change. (Figure 9b) Therein, the thermally activated "hopping" part was used to determine $W_B$. This was determined to be 11.3 K or 1 meV. Thus, the free carriers and Hall mobility could be deduced. For didactic purposes, the number of free carriers was normalized to the monomer-density in the film. For this, a density of 1.55 g cm$^{-3}$ (obtained from Rutherford scattering) and a molar mass, M, of 174 g mol$^{-1}$ was assumed (based on a doping ratio of 1:2.8 obtained from XPS data). (Figure 9c) The Hall measurement was done on the sample shown in Figure 9d. The polymer was scratched-off the sapphire substrate in order to avoid measurement errors in electron transport properties and covered in polymethylmethacrylate (PMMA) to avoid degradation by external influences. Note, that the metallic contacts were still functional despite appearing differently.

### 7.1.5. Optics

In the context of transparent electrodes, the optical performance of a material is paramount to commercial success. Additionally, optical properties can yield information about polymerization (IRAV-bands), ellipsometry can probe the metallic state (Drude tail). Optical measurements were done on 155 nm thin films. Polarization measurements were done via ellipsometry on 40 and 100 nm thin-films.
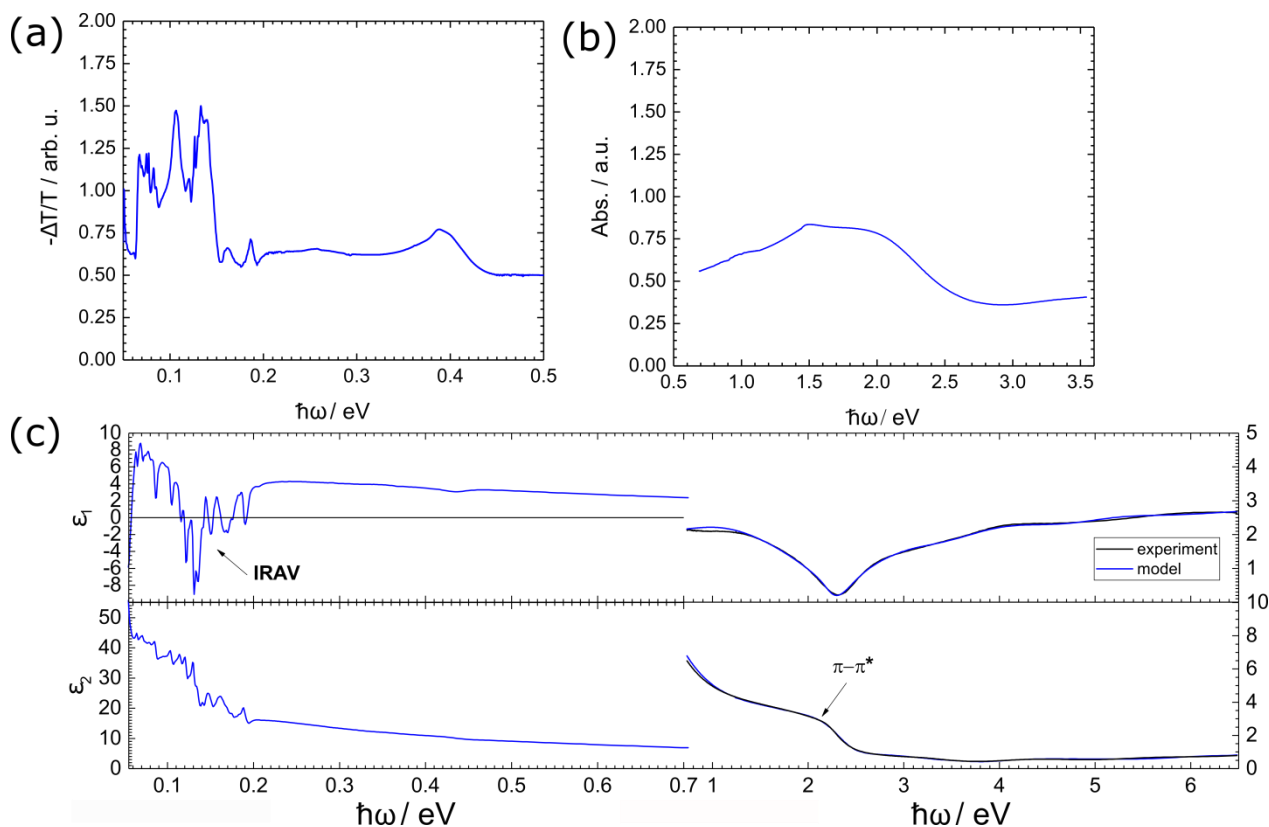


Figure 10: Optical measurements of PEDOT:sulphate of ~40 nm thin-films.[6] (a) ATR-FTIR measurement. Note the IRAV band in the range of up to 0.17 eV (~1400 cm$^{-1}$) typical for polymers. (b) Absorption spectrum corresponding to a blue material. (c) Elispometry measurement in the IR and UV-vis region modelled from measurements at angles from 55-85 °. Theory and measurement are in good agreement with each other, spectra are Krames-Kronig consistent. Polarisation in the low-energy region of $\varepsilon_2$ indicates the presence of a Drude tail, meaning a true metallic charge carriers being present in the film.

The optical properties of PEDOT:sulphate were investigated in the IR and UV-vis regions. ATR-FTIR measurements were conducted revealing typical features of a conducting polymer, the IRAV bands. (Figure 10a) The strong absorption around 0.4 eV (~2800 cm$^{-1}$) corresponds to the presence of OH groups, owed to the presence of hygroscopic sulphate ions.

Reflection corrected absorption spectra in the UV and visible spectral region show a broad absorption at lower energies and absorption minimum owed to the typical disperse blue colour of PEDOT. (Figure 10b) The absorption shows multiple shoulders and no precisely defined maximum. This is in good agreement with MALDI-MS, where a distribution of chain-lengths was found to be present in the material.

Ellipsometry measurements were conducted to investigate the polarisation response. (Figure 10c) The measured spectra and the model are in good agreement, the latter being Kramers-Kronig consistent. The expected π- π* transition is observed, however, the polaron-transitions were weak to the point of being hardly observable. On the other hand, a strong, Drude-tail-like

feature was observed in the $\varepsilon_2$ spectrum was observed, supporting the metallic features observed earlier in the charge transport experiments.

## 7.2. PEDOT:sulphate thick films under hydrostatic pressure

After observing strong indication for a metallic system, we intended to further press our argument of structural order and enhance the metallic state throughout the sample. Thick-films were used as we needed the mechanical stability of free-standing films. As a side effect of that, the physical properties would be expected to be closer to a bulk-specimen (3D) rather than to a thin film where, at least hypothetically, more boundaries and thus disorder, would be expected. The herein shown results were published elsewhere by the author and are referenced accordingly.[71]
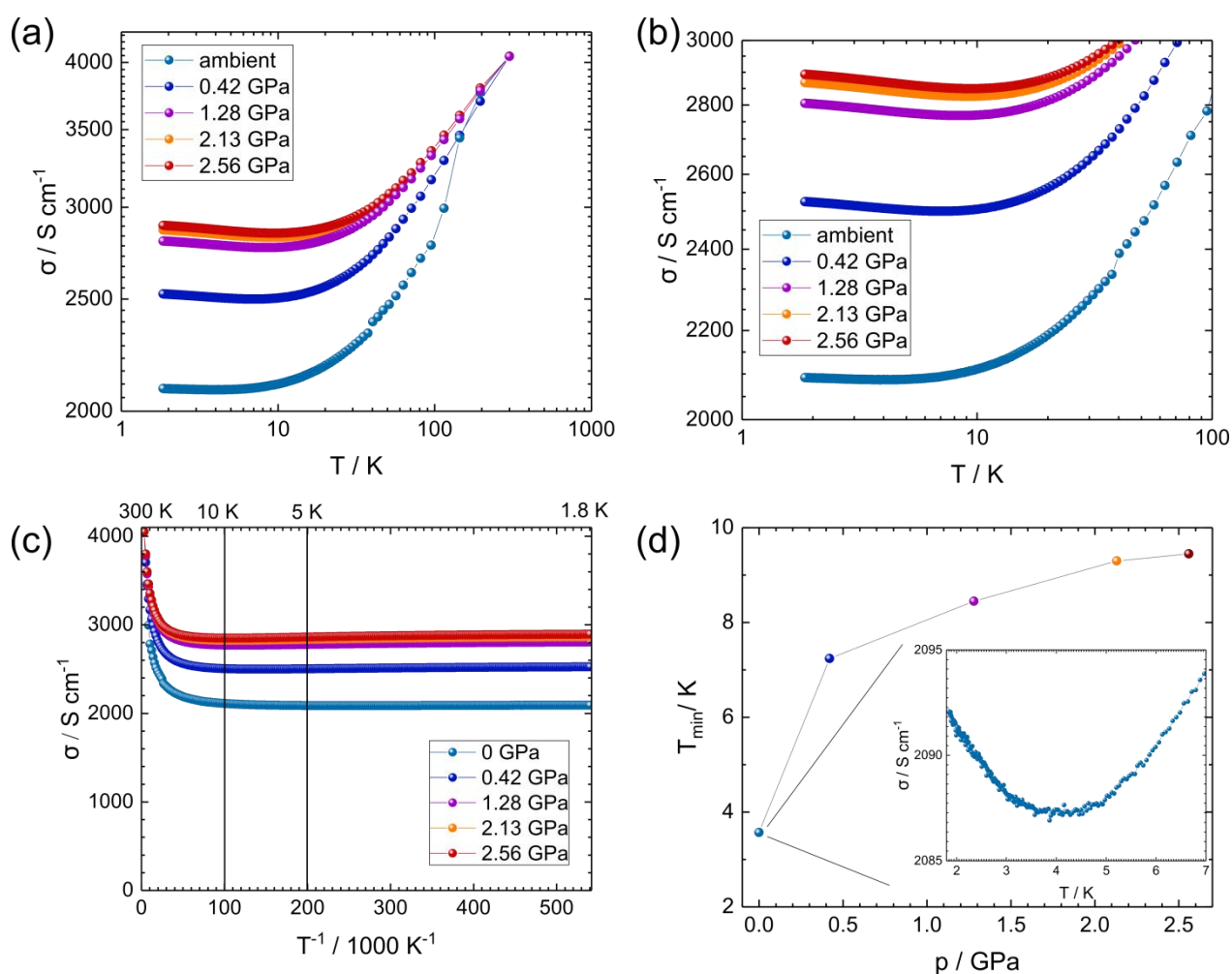
### 7.2.1. Charge carrier transport



Figure 11: PEDOT:sulphate free-standing, thick films measured in a hydrostatic pressure cell.[71] (a) Temperature dependent conductivity measurements in 4-probe configuration at different pressures. Note the conductivity minimum appearing at temperatures up to 10 K. (b) Zoom at the low-T region. (c) Reciprocal temperature comparison of conductivity measurement at different pressures. The non-pressurized samples exhibits about 52% of conductivity retention. (d) Conductivity minimum beyond the Mott minimum at various pressures in comparison. (colour coded for pressure) The strongest effect is seen at the lower load pressures.

Temperature-dependent conductivity measurements were conducted for thick-films in the same way as for thin films shown in the previous chapter. In this case, however, the parameter of load-pressure was varied. (Figure 11a-c) Note, that the temperature is plotted in a log-scale in order to enhance the low-temperature range. Similarly as in thin-films, the thick films exhibited metallic finger-prints in their behaviour. Unlike the thin-films, however, a conductivity minimum was observed for all pressures, including load-free conditions. This is a rare phenomenon in

conductive polymers.[47,74–77] Interestingly enough, the conductivity retention at low temperatures was less pronounced, but would be enhanced by pressure. The retention at ambient pressures was about 52% and would increase to 72 % at 2.56 GPa. The reason for that discrepancy remains elusive.
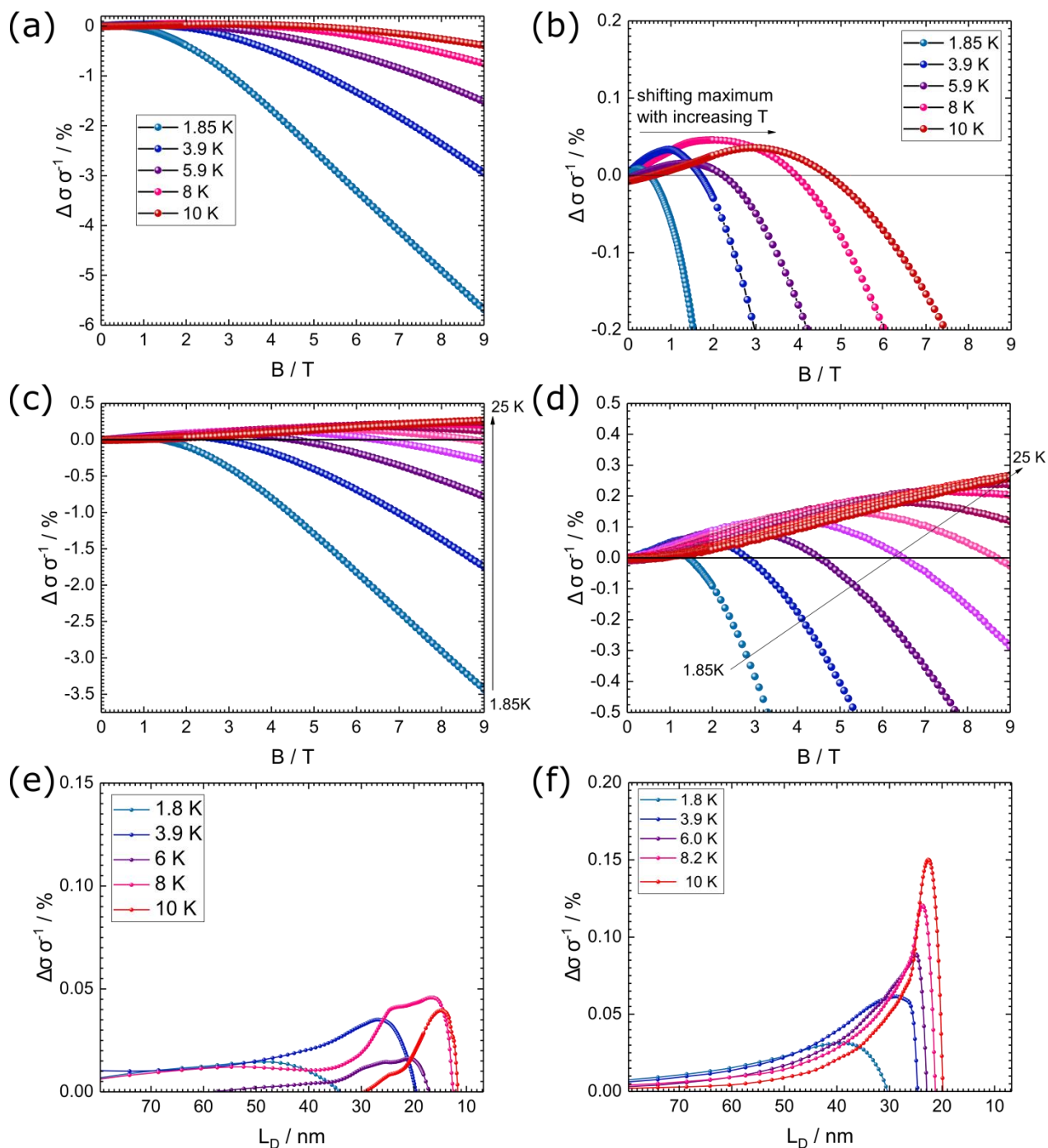


Figure 12: Magnetoconductivity measurements on pressurized PEDOT:sulphate.[71] (MC) measurements and their evaluation for PEDOT: sulphate at for ambient and 2.56 GPa load pressure.(a) MC measurement for ambient pressure and various temperatures. (b) Zoom on the positive MC. (c) MC measurements for a load pressure of 2.56 GPa. (d) Zoom on the MC at 2.56 GPa. The maximum in MC cannot be reached at temperatures above 20 K with our setup anymore. (e) Ambient pressure measurement reformulated to show the scattering length in form of the Landau orbit size (~scattering length). (f) Ambient pressure measurement reformulated to show the scattering length in form of the Landau orbit size (~scattering length).

We should now focus on the effect on pressure on the conductivity minimum (Figure 11d) The minimum was observed to shift with applied pressure- the higher the pressure, the more it would wander. It would, however, saturate towards temperatures of 10 K.

As expected from a typically metallic sample, MC measurements revealed the typical interplay between MC and ML. Here, we will focus on ambient pressure (Figure 12a,b) and 2.56 GPa (Figure 12c,d).

At ambient pressures, a picture similar to thin-films was obtained, with the maximum consequently shifting to higher temperatures. (Figure 12a,b) The picture was less smooth when the results were reformulated into the Landau orbit size, where only at 1.85 K a single peak (49 nm) was observed. (Figure 12e) At higher temperatures, the orbit size would shrink and a shoulder would manifest. This would mean, that two resonances, *i.e.* delocalization lengths or types of scattering were present in the sample. With warming-up, the sample, the higher-length would start to diminish. Because of this observation, we would focus on scattering effects, later. (Figure 13)

At elevated load pressure (here, 2.56 GPa, Figure 12c,d), again, an interplay between MC and ML was observed- the signature of metallic polymers. With our instrument, distinct maxima were observable only for temperatures below 20 K. Above that, the magnetic field was not able enhance electron-electron interactions enough to induce strong-enough localization. Reformulating into the Landau orbit size (Figure 12f), the observed resonances were much more expressed, indicating that a more uniform delocalization was achieved. This can be explained by a better overlap between molecular orbitals. Keeping in mind the XRD and TEM data, the scattering length was in the order of crystallite size. Whatever effect would effect it, was strongly appearing to be an intra-crystal effect and not passing beyond the crystals boundary.

The analysis of the effects of the complex system of conductivity versus pressure and temperature on scattering length was attempted and proved highly complex. (Figure 13a-c)

First, the effects of pressure at constant temperature were analyzed. (Figure 13a) At any temperature apart from 1.85 K, a dramatic increase of scattering length upon pressurization would be seen, followed by a slow decrease or stagnation. This would normally indicate a transition from one effect to another. At the lowest investigated temperature, however, the scattering length would monotonously decrease, indicating the absence of a transition.

Second, when the problem is observed at constant pressures, an interesting discrepancy of scattering-length-saturation upon heating is observed. (Figure 13b) At ambient pressure and 1.85K, the systems delocalization length is the farthest and becomes lower the higher the pressure. Thinking along the lines of disorder, it could be argued that the effect of cooling corresponds to a slow, gradual, and more ordered way of compression as it would have a much more visible effect on enhancing the scattering length. Besides this, the presence and absence of pressure would be most expressed at 10 K. At all the elevated pressures, the scattering length would approach 22 nm at 10 K, while at ambient pressure this value would be only around 15 nm. This indicates, that pressure contracts the samples and keeps the orbital-overlap between single strands high, even at elevated temperatures.

The effects of pressure on scattering remained inconclusive until the data were correlated to conductivity measurements. (Figure 13c) The more elastic type of charge transport the shorter scattering lengths would be expected. (Figure 13a, 1.85 K) At higher temperatures at the transition from absent to "low" load pressures, however, this picture becomes less clear- at the same where conductivity is affected the strongest by pressure. As the pressure effect on conductivity saturates, the same occurs in the context of scattering length. We believe that this effect corresponds to a pressure-induced transition from inelastic to elastic scattering.
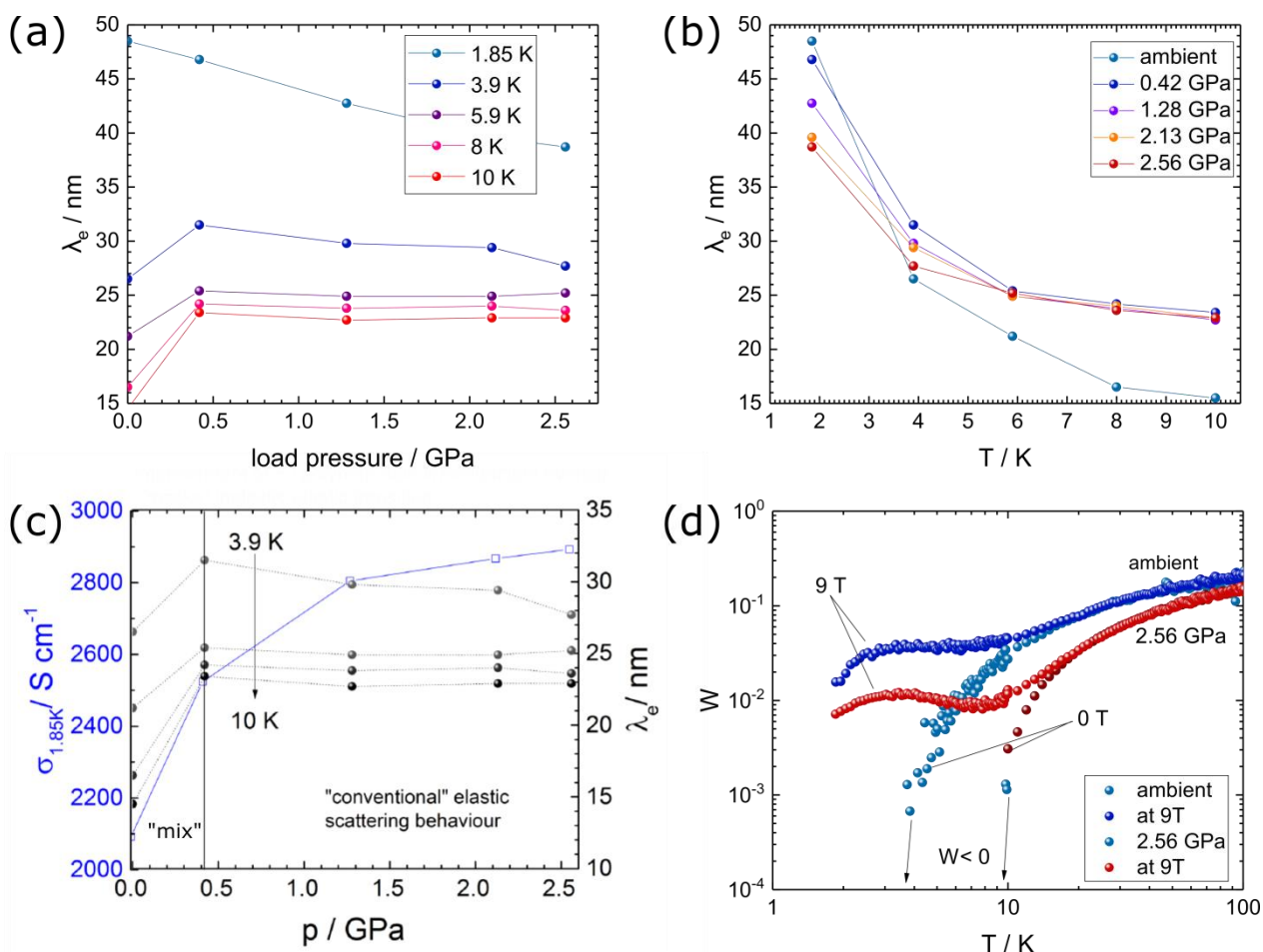
Figure 13: Transport trends in PEDOT:sulphate relative to load pressure.[71] (a) Pressure effect on the scattering length at different temperatures. (b) Temperature effect on the scattering length at different pressures. Note, that upon pressurization, the scattering length at higher temperatures unifies. The high-T delocalization at the absence of pressure is significantly worse, however, grows much faster upon cooling. (c) Comparison of pressure effect on scattering length with conductivity change at 1.85 K. (d) W-plots for ambient and maximal load pressure. The conductivity minimum manifests here as a transition to negative values (undefined in a logarithmic function)

Beside scattering effects, we observed the MIT for ambient and pressure loads of 2.56 GPa. (Figure 13d)

In the absence of a B-field, both showed behaviour typical for a glassy metal and a transition to crystalline metal behaviour at around 4 or 10 K, respectively. At ambient conditions, a magnetic field of 9 T quenched the metallic state and transferred the system to the critical regime of the MIT. Only below 3 K, the system reverted back into the glassy metallic regime.

At elevated pressure, a B-field of 9 T resulted in a transition not only into the critical, but the insulating regime! Still, at roughly 3 K a reversion to the glassy metallic regime would occur. This indicates, that the metallic state in PEDOT:sulphate is especially strong and cannot even be permanently quenched by a strong magnetic field- cooling to lower temperatures will always cause an MIT.

## 7.3. PEDTT: sulphate

PEDTT and PEDOT are different, despite being structural analogues- the consideration to that are shown in the corresponding experimental (synthesis) and theory part.

Both materials could be easily removed off a substrate by scotch-tape and would easily delaminate from a glass substrate unless it was pre-treated by a SAM of OTS.

Classically, PEDTT was long ago determined to be a "bad" conducting polymer, mainly because of the missing intra-molecular interaction of S-O bridges.[41–43,70] In the following chapters, we will challenge some of the logic made paradigm and confirm other parts of the hypotheses.

The previous conductivity record for PEDTT was set already when it was first published in 1995, which was 0.4 S/cm.[78] To reach that, a strong oxidant ($ClO_4^-$) was necessary.

The data presented herein are currently prepared to be published in a separate manuscript.[79]

### 7.3.1. Charge carrier transport

Measuring conductivity in PEDTT:sulphate, a substantial difference to PEDOT was observed. First of all, the conductivities reached were on the range of commercially available, processed PEDOT:PSS (PH1000)[11] yet not as good as in PEDOT:sulphate (1050 S/cm at room-temperature). In the reference system of PEDTT-based materials, this represents a 2600-fold improvement in conductivity over the previous record from 1995.[78]

Charge-carrier transport measurements revealed some other interesting effects. (Figure 14)



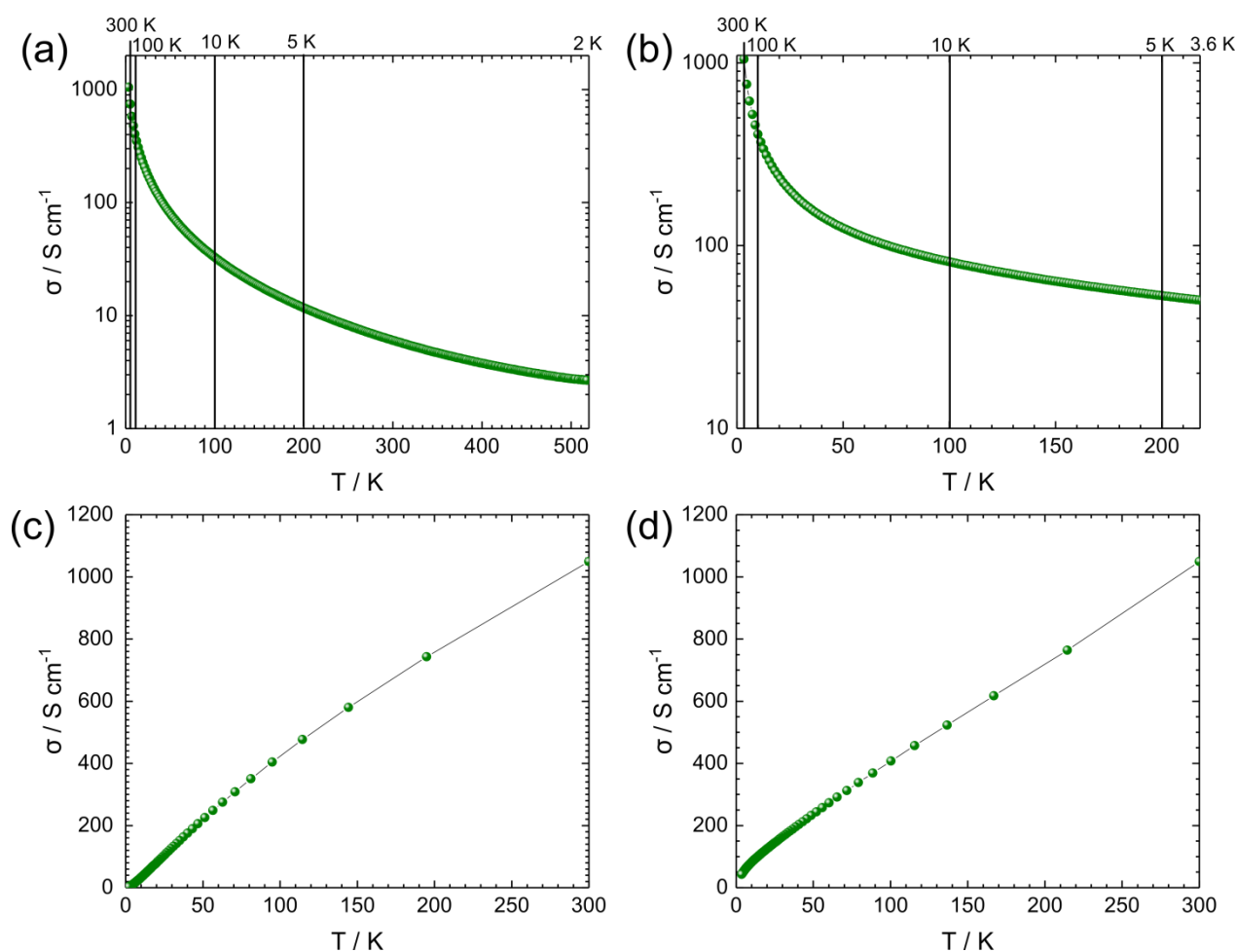Figure 14: PEDTT:sulphate conductivity measurements.[79] The minimal temperature was limited by the instruments cooling capability. (a) 400 nm thin-film, conductivity versus reciprocal temperature. (b) 150 nm thin-film, conductivity versus reciprocal temperature. (c) 400 nm thin films conductivity measurement versus temperature. (d) 150 nm thin films conductivity measurement versus temperature.

Based on previous experience with the effect of thick and thin films, we decided to investigate thin-films of different thicknesses, namely 400 and 150 nm.

Comparing conductivity in reciprocal Kelvin, an interesting difference was observed. (Figure 14a,b) Though conductivity in both samples at room-temperature was similar, they temperature dependence was different. We can clearly annotate this effect to the disorder: the farther from the substrate the material is deposited, the less ordered it becomes. In other words, we can observe an epitaxial effect from the sapphire substrate.

The conductivity profile plotted directly against temperature can be seen in Figure 14c,d. What becomes immediately clear, is that the retention of conductive properties is in both cases significantly lower than in PEDOT, namely, 1% and 5% at 3.6 K for the 400 and 150 nm film, respectively. This would further sink to 0.3% in the thicker sample when approaching 2 K. This indicates that the samples would not undergo an MIT- the observed behaviour rather appears like that of a material in the critical regime.
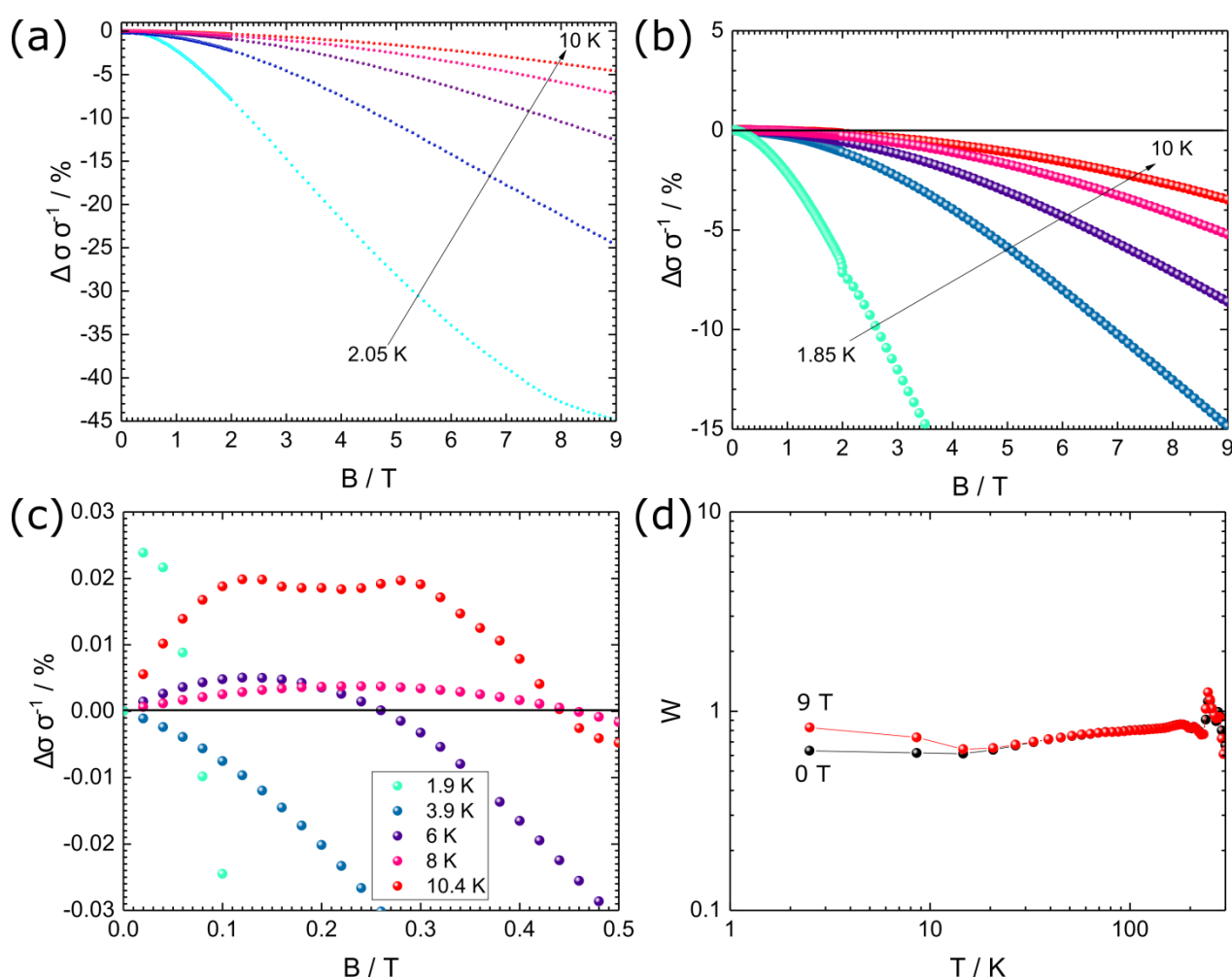


Figure 15: MC measurements of PEDTT:sulphate.[79] (a) Conductivity measurements with a magnetic field applied in a 400 nm thin-film. Only ML was observed, hence no metallic behaviour. (b) Conductivity measurements with a magnetic field applied in a 150 nm thin-film. (c) Zoom on conductivity measurements with a magnetic field applied in a 150 nm thin-film. A sort of MC-effect was observed at very low fields, *i.e.* considerably below 0.5 T.(d) W-plot in 150 nm thin films. A B-field of 9 T forces a transition from the critical to the insulating regime.

When a magnetic field was applied during the conductivity measurements, the effects observed in the 400 nm film were quite unremarkable. (Figure 15a) Only ML was observed, the system clearly insulating as the disorder introduced during longer synthesis runs would strongly affect the whole film.

In the 150 nm films, a different situation was observed. (Figure 15b, c) There, a extremely weak MC-effect was observed at very low fields. (below 0.5 T) The metallic state, if present at all, appears to be fragile and easily quenched by strong fields. Further, we have observed a series of anomalies relative to PEDOT: at 3.9 K, no MC effect was observed at all. At 6 and 8 K, the MC was minimal and only at 10 K, a similarly strong effect was observed. It can be argued, that this could be caused by an underlying magnetic effect. The measurements were done by starting at the lowest temperature and then scanning the magnetic field from 0 to 9 T. If the critical temperature was located below 6 but above 3.9 K, the state induced by a B-field of 9 T at 1.9 K would still be present at 3.9 K. A similar yet weaker suppression would occur in the 6 and 8 K scans.

Also, at 10 K in MC a twin-peaks at 0.14 and 0.28 T were observed. This effect is unusual yet fits the theory[53]: an interplay between positive and negative MC is observed. The presence of two peaks could be explained by various delocalization lengths or scattering mechanisms dominating in the material.

As the 150 nm thin-film appeared to show latent metallic features, the data were transformed into a W-plot. (Figure 15d) In the absence of a magnetic field, the material was clearly in the critical regime of the MIT. As observed earlier in MC, the materials charge-carrier transport properties show a susceptibility to strong magnetic fields. Indeed, at 9 T, a transition from critical to insulating regime was observed.

Observing conductivity and MC measurements in PEDTT: sulphate, we can hypothesize that not only the counter-ion but also the structural support by the substrate plays a crucial role in enhancing the metallic state. Therefore, optimization of the substrate or the use of an interlayer might still enhance the conductive properties. This, in turn, would indicate a direct connection between structural properties effected by the substrate (*i.e.* an epitaxial effect) and the resulting electronic properties.

### 7.3.2. Structural order and Chemical Identity

The transport properties observed raised a lot of questions, mainly what caused the high conductive properties and the MC-effects on the verge of metallic conduction.
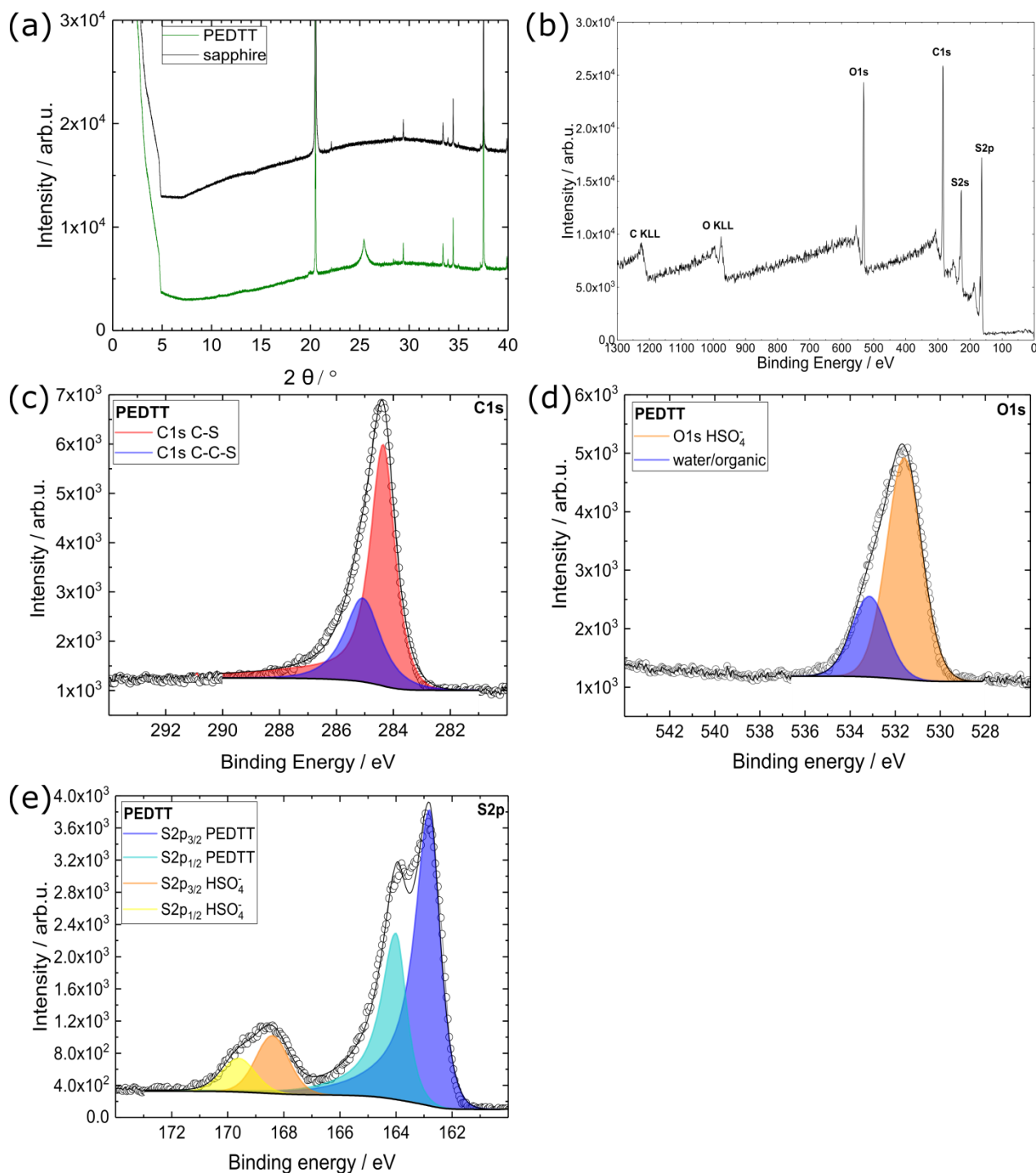


Figure 16: X-ray data on PEDTT.[79] (a) XRD on sapphire. Peak at 25.5 ° corresponds to a crystal size of 35-50 nm and a stacking distance of 3.6 å. (b) XPS survey scan revealing O, C, and S. (c) C1s spectrum. Two signals, one from the thiophene-ring, the other the possibly from the ethyl-carbons connecting the side-group thioether groups. (d) O1s spectrum. Additionally to the expected contribution from sulphate, another, unknown signal was found. From the binding energy it could correspond to water or an alcohol. (e) S2p spectrum. Two twin peaks (1/2 and 3/2 contribution) of sulphate and PEDTT. The presence of

Previous literature would suggest that the material can be a latent conductor at room temperature- temperature dependent measurements were never attempted, conduction in the

critical regime of the MIT, let alone metallic properties, were never even considered. The question was, what was causing these exact properties in PEDTT:sulphate. Also, it was to be shown that the chemical identity of the material was actually said polymer.

In order to answer these questions, XRD and XPS were performed, both revealing information crucial to understand the electrical properties.

First, XRD measurements were performed (Figure 16a), revealing a strong response around 25.5 °. As there is no previous literature on XRD on PEDTT, we were not able to annotate a specific face to the peak. The Scherrer formula indicates a minimal crystallite size of 35-50 nm (depending on parameters), the stacking distance is similar to PEDOT and was determined to be 3.6 å. From this, we suggest that a similar type of dopant-polymer intercalation would be present as in the case of PEDOT.

Additionally to XRD, XPS spectra were conducted to learn more about the chemical state of the material. A survey scan revealed elemental purity, just as in PEDOT, and suggested the presence of oxygen (21%), carbon (51%), and sulphur (27.8%). (Figure 16b) The absence of a gold-signal indicates pinhole-free coverage of the substrate.

Focusing on C1s (Figure 16c), two contributions were revealed, one corresponding to the carbon in the thiophene ring (4 C of similar binding energy due to conjugation), the other having its origin in the ethyl-group of the thioether (2 equivalent positions). The ratios of these two were found to be 70.1:29.9 (atom%), which is in good agreement with the 66.6:33.3 expected from PEDTT.

High resolution data on O1s not as neat. (Figure 16d) In PEDTT:sulphate, the only oxygen contribution would be from the counterion. On the contrary, close to 30% were from an adventitious source. This would either suggest the presence of an organic source or the adsorption of water to the film. In the absence of the corresponding signal in the C1s spectrum, water remains the sole explanation.

In the S2p spectrum, two contributions, from PEDTT and its counterion, are present. (Figure 16e) From this, a 1.67 subunits of the polymer are present in the film per sulphate or hydrogensulphate. This is in good agreement with the calculation from oxygen levels (1.58:1).

Despite the apparently high degree of doping, it is necessary to keep in mind that the ratio in the top 10nm might well be overestimated as adsorption is an issue. Revisiting the lessons learned from PEDOT suggest that a 3-fold overestimation is well possible. XPS revealed a 2.8:1 monomer:dopant ratio, while an actual 10:1 doping was measurable in the way of the Hall effect.

### 7.3.3. Optical properties

So far, we know that PEDTT:sulphate is a green material in the critical regime of the MIT. As material production on a scale needed to perform MALDI-MS was not feasible, ATR-FTIR was relied upon. Further, ellipsometry (on 26 nm thin-films) was to reveal, if it could reveal the presence of metallic electrons, *i.e.* a Drude tail, just as in PEDOT:sulphate. ATR-FTIR and UV-vis absorption were both recorded on 150 nm thin-films.
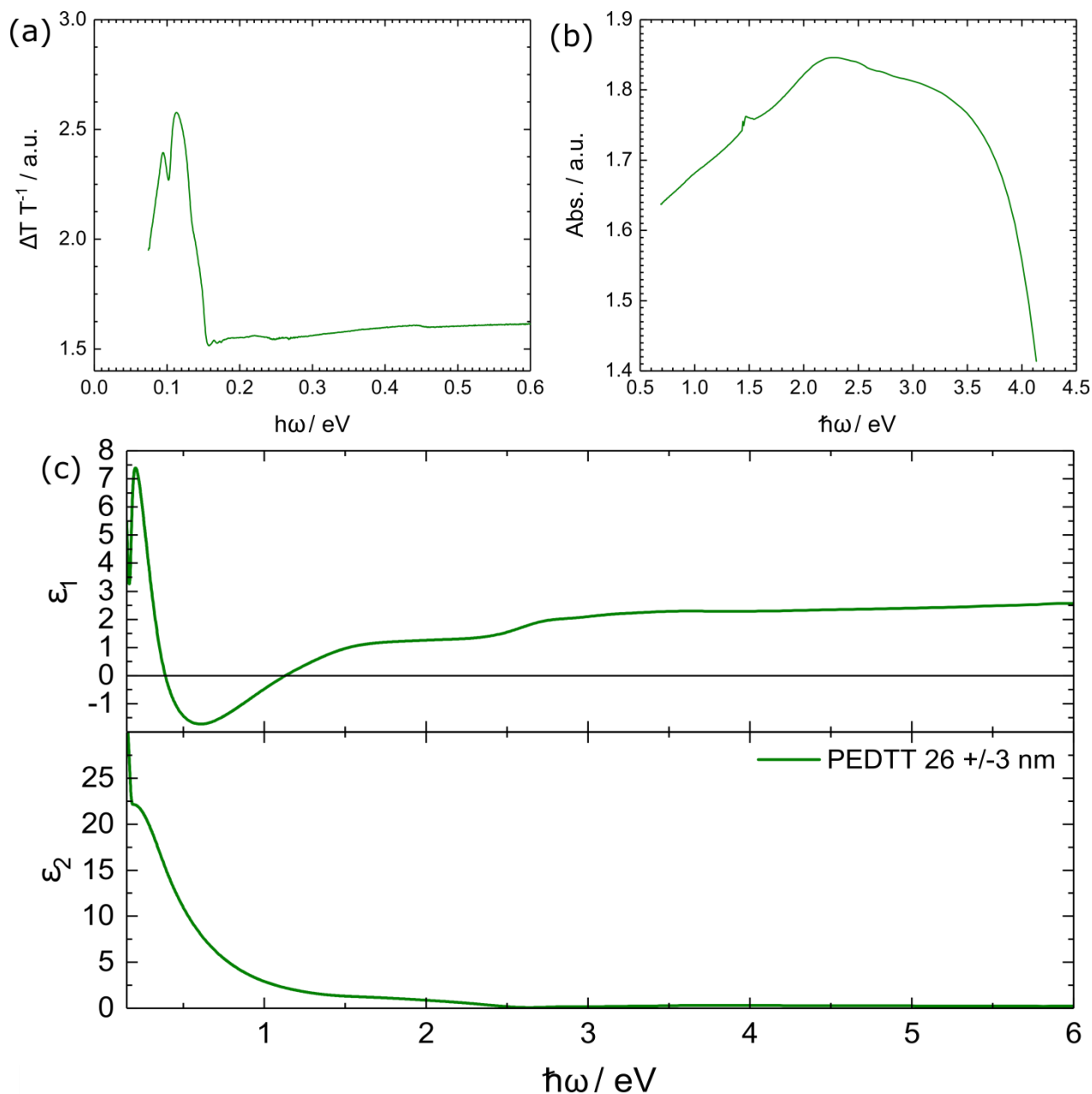
Figure 17:Optical properties of PEDTT:sulphate.[79] (a) ATR-FTIR spectrum. The spectrum gives results similar to an absorption measurement and exhibits strong IRAV-bands below 0.15 eV. (~1300 cm$^{-1}$) (b) UV-vis absorption spectrum. (c) Ellipsometry polarization spectrum modelled from measurements at angles from 55-85 °.

Measuring the ATR-FTIR spectrum revealed the presence of IRAV-bands, hence an indication of polymerization. (Figure 17a) Further, a weak contribution around 0.4 eV (~3200 cm$^{-1}$) suggests that water is present.

The UV-vis absorption spectrum was measured. (Figure 17b) A broad absorption was observed with its maximum at 2.3 eV. The presence of shoulders to both sides suggest different absorbing systems being present (*i.e.* different chain-lengths), just as in PEDOT:sulphate.

Ellipsometry measurements were conducted in order to better understand the polarization effects in PEDTT. (Figure 17c) For this, a clean microscopy slide (rough on the backside) was inserted into the tube-reactor and PEDTT was grown on top of it. The spectra were in good agreement with each other, meaning that optically equivalent material was deposited throughout the deposition zone. The results are Kramers-Kronig consistent. Interestingly, below 0.18 eV, phonons typical for glass would grow very intense, strongly interfering with the measurement. Therefore, data above this energy are shown.

Unlike in PEDOT, it was not possible to detect a Drude tail PEDTT, *i.e.* no charge-carrier delocalization was determined. The Drude-like contribution is actually caused by the materials doping.

Simulations of the sample thickness suggested a weighted mean-roughness of 150%. For imagination, this would suggest an archipelago-like situation similar to the one observed in PEDOT:sulphate: here instead, sharp peaks on the range of several tens or hundreds of nanometers amidst a "sea" of thinner material. Correlating these findings with the observations done in PEDOT, it can be argued that the sharp features represent structurally ordered, crystalline material, whereas the thinner layer presents disordered domains. This would be in good agreement with the findings from XRD.

## 7.4. PTP:sulphate

Polythieno[3,4b]pyrazine (PTP) is the farthest "relative" in the list of polymers investigated in this thesis- and not only in name. It was first reported in 1995.[80] The main difference to PEDOT and PEDTT lies in the fact that the pyrazine ring exhibits aromatic properties and therefore presents two reactive sites not present in its structural analogues. (see Chapter 6.7) Literature therefore always mentions PTP (in non-theoretical work) with alkyl-protection groups for the non-thiophene reactive sites.[80–85]

Despite protecting groups and serious synthetic optimization, the conductivity record was established only in 2007: $1.95 \times 10^{-5}$ and $3.75 \times 10^{-3}$ for the C7 and C12 protected monomers, respectively.

Despite being prepared in the same way as PEDOT or PEDTT, and theoretically being a structural analogue thereof, it differs greatly. Strong mechanical interaction with glass similar to polydopamine was observed.[19,86] The material would not delaminate nor be removed by scotch-tape, once deposited. The charge-carrier transport properties, however, would not even remotely compete with those of PEDOT or PEDTT.

### 7.4.1. Charge carrier transport

Transport properties of PTP were always previously advertised to be non-ideal to say the least. Multiple repetitions left us with a record in the range of 0.5 S/cm. In comparison with the previous record a significant advantage. It should be noted, that temperature-dependent measurements cannot be reported as no ohmic contact could be established. Current/voltage (I/V) curves would not be linear but show an S-shape, even in the pA, similar to measuring a sample covered in a thin layer of conductive liquid. Attempts of drying the surface remained unsuccessful.

### 7.4.2. Chemical Identity

In order to understand reactivity and therefore chemical identity of PTP, XPS was conducted. It revealed the presence of elements and their chemical states.

The survey scan revealed the presence of O (37.4 at%), N(11.0 at%), C(37.7 at%), and S(14.4 at%). (Figure 18a) This already indicates an increased content of sulphuric acid or sulphate. (1:2 ratio of PTP to "dopant") Additionally, an adventitious source of sodium (Na) was found, suggesting that this was coming from an imperfectly covered substrate. (as sodium cannot be a pollution from oCVD due to its negligible vapour pressure)

The high resolution C1s scan revealed 46:23 ratio of thiophene carbon to the ethyl signal. (Figure 18b) Unfortunately, another intense signal (25.7%) and less intense (5.3%) was present. The latter can be attributed to adventitious carbon adsorbed to the material. The stronger signals shift corresponds to C-C/C-H. In the absence of available literature, an educated guess would suggest oxidative damage, side-reactions on the pyrazine-ring, pollution by an unknown contaminant, or a combination of all of these being the source.

High resolution scans for sulphur revealed two distinct signals, one for PTP, the other for the dopant. (Figure 18c) The ratio of both contributions confirmed the previously determined ratio. The source of so high "dopant" contents suggests the adsorption of large amounts sulphuric on the

Probing for nitrogen, N1s high resolution scans were performed. (Figure 18d) The main contribution (60.9 at%) corresponds to the unpolymerized pyrazine-ring. On the other hand, two more signals designated comp1 and comp2 of 34.6 and 4.5 at%, respectively, were present.

From the chemical shift we suggest that comp1 could be the expected side reaction on the pyrazine ring, the other is in the range typical for an N-H group.
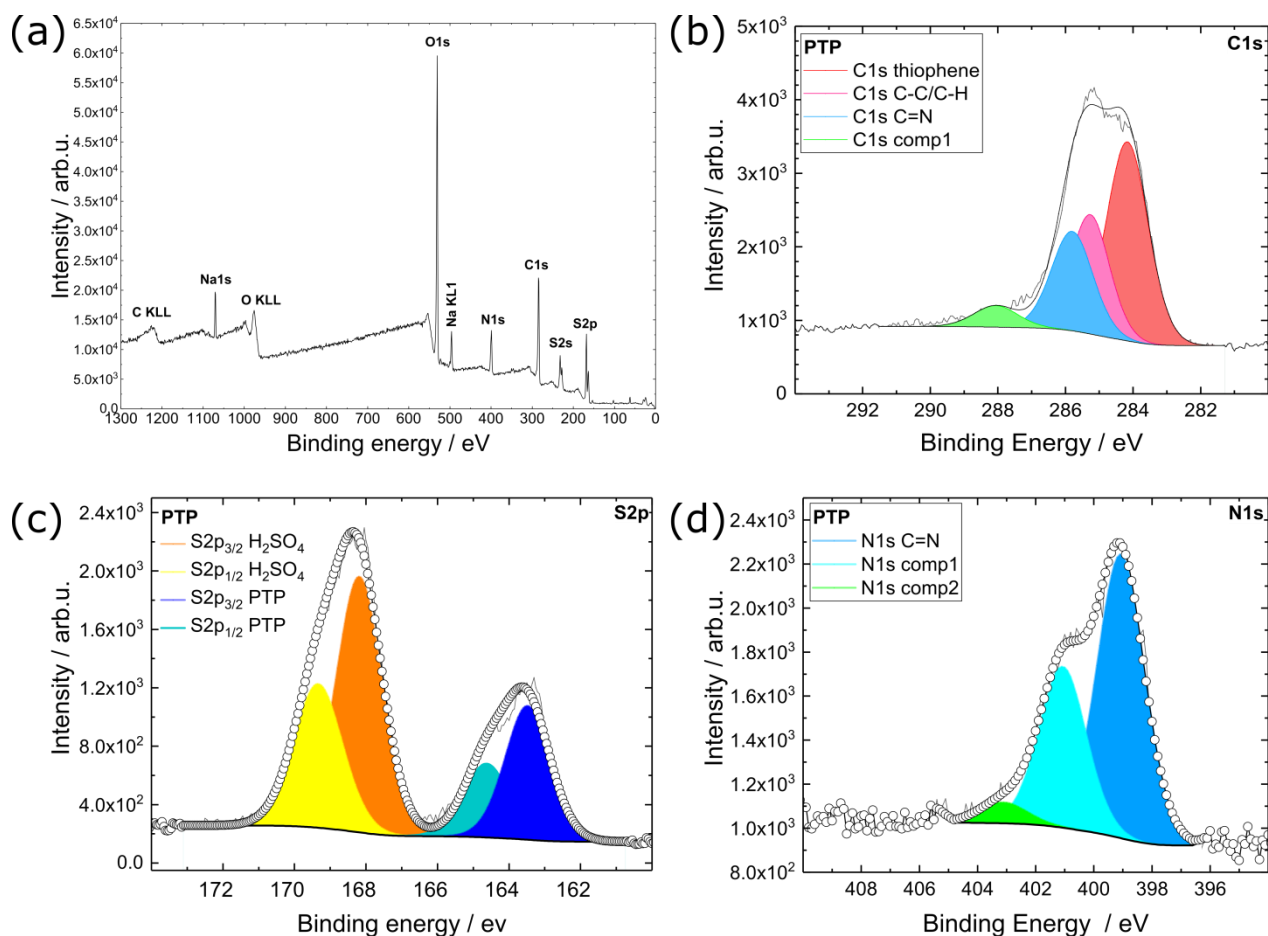


Figure 18: XPS spectra of PTP.[87] (a) Survey scan revealing the presence of Na, O, N, C, S. The presence of sodium indicates pollution from an unknown source. (b) C1s spectrum. Additionally to the signal of carbon incorporated in the thiophene-ring and C-N from the pyrazine ring, an additional signal corresponding to C-C/C-H was present. This might be interpreted as the presence of a side reaction of the pyrazine ring. Comp 1 corresponds to adventitious carbon. (c) S2p spectrum. A substantial amount of sulphuric acid (see ATR-FTIR results) was found to be present. (d) N1s spectrum. Additionally to the expected C=N contribution, two more components were observed. The higher energy component could be an oxidized feature, the lower energy component could be a shift due to the aforementioned side-reaction.

The consequence of these results suggests not only that a polymerization different from the chain-like structure that we observed in PEDOT and PEDTT would occur. Due to that, structural ordering observable (in XRD) in PEDOT and PEDTT and consequently good orbital overlap and intermolecular electron movement becomes nigh impossible.

Another consequence is the formation of a highly porous. This volume could then, theoretically, be occupied by liquids, such as electrolytes, which is in turn explaining the S-shaped I/V-curves. Consequently, the measured conductivity may well be overestimated and should be seen with caution.

### 7.4.3. Optical properties

Given the inferior properties of PTP as a conducting polymer, optical measurements presented a simple way of gaining more information on the reason why that was so. (Figure 19)
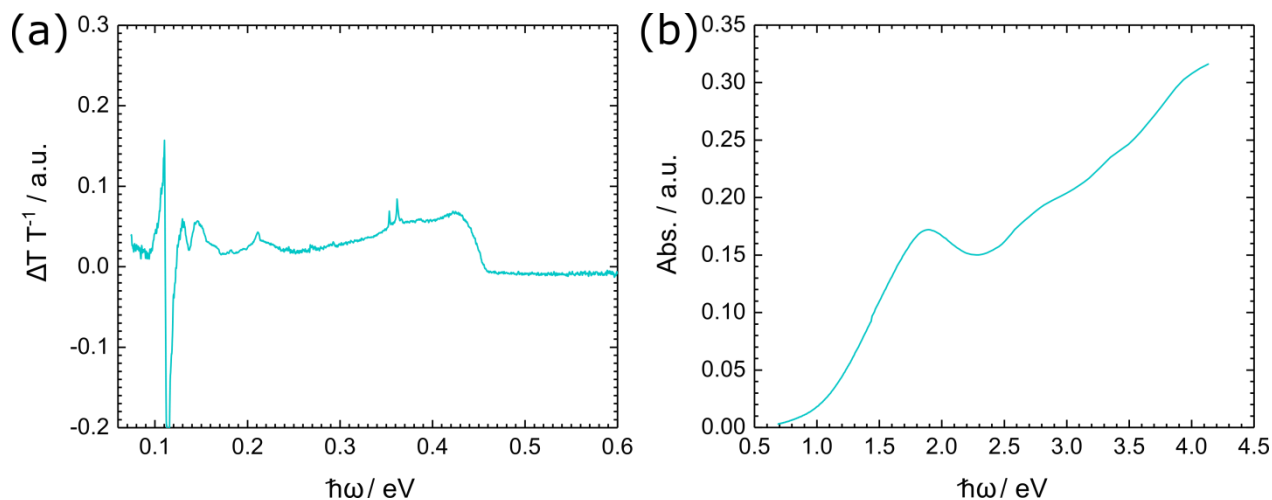


Figure 19: Optical spectra of 56 nm thin film of PTP.[87] (a) ATR-FTIR of PTP. Most importantly to point our are the IRAV bands below 0.17 eV (~1400 cm$^{-1}$) and the strong, broad absorption around 0.42 eV, corresponding to the presence of O-H functional groups in the sample. (b) UV-vis absorption spectrum. Two sets of absorption are apparent with a minimum around 2.3 eV, corresponding to a green/slightly blueish material. This is in good agreement with the actual colour which was turquoise.

ATR-FTIR spectra were recorded off 56 nm of material deposited on glass. (Figure 19a) Strong IRAV bands were observed as well as a strong absorption of O-H vibrations. This typically corresponds to the presence of water. Given the information of XPS spectra, this actually corresponds to sulphuric acid. This bring further doubts about the credibility of the conductivity measurement.

The same film was used to measure UV-vis spectra. (Figure 19b) The material has a strong absorption in the IR on the verge of the visible region. The minimum at ~2.3 eV (~540 nm) corresponds to a turquoise colour, well in agreement with the observable colour. Further, the absorption would increase with photon energy, showing multiple shoulders, indicating different species contributing to the optical properties. This is in good agreement with our hypothesis of side-reactions such as branching occurring during synthesis.

## 8. Conclusions

Conductive polymers are researched for a long time and great progress was made over the years. In the scope of this thesis, it was attempted to contribute to that field by taking a novel approach.

Deciding to value simplicity over complex, work-intensive design, a novel implementation of oCVD was successfully developed, combining film deposition, doping, and as a prerequisite for these, also synthesis, into a single step. By widely eliminating the possibility of human error, synthesis and characterization for three distinct thiophene systems were achieved.

The use of sulphate as a counter-ion showed intrinsic advantages as it facilitated integration into the polymer matrix without disrupting π- π-stacking (size effect). Additionally, sulphate-salts have a tendency to form large crystallites, which is why they are relied upon in high-school experiments to demonstrate crystal-growth. In PEDOT and PEDTT, we were able to exploit this exact property to form extraordinarily large crystallites (on the range of tens of nanometers).

For PEDOT, evidence for metallic properties was presented, with a conductivity minimum in thick films. This in itself presents a great contribution to the field as it creates a case of precedent and could possibly promote research going in the direction of metallic polymers or in future even polymeric superconductors.

Also, electron scattering studies and showing the presence of a measurable Hall effect in a material doped by mild oxidizing agents (in the context of the field) opens new horizons to the understanding of this complex matter.

In the case of PEDTT, the achievements seem to be much less prestigious as they are dwarfed by those in PEDOT:sulphate. On the contrary, they are of much greater consequence. They present groundbreaking achievements as they contradict predictions and the rationale made decades ago.

We demonstrated that the counter-ion plays a much greater role in the film than removing electrons. In the case of PEDOT:PSS, it delivers advantageous mechanical and adhesive properties, which are well known. In PEDOT:sulphate, the counter-ion acts as a crystallization agent that does not influence π-stacking. In PEDTT:sulphate, the small counter-ion, however, plays an even greater role. It stabilizes and flattens the polymer structure and delivers a crystalline system with similar stacking distances thus facilitating electron conduction, and delivering a material in the critical regime of the MIT. In this way, a 2600-fold improvement in room-temperature conductivity was achieved, turning a semiconductor into a conducting system of more than 1000 S/cm! Even at low temperatures (2 K), finite conductivities were measured.

An interesting fact that needs to be revisited are the MC-effects encountered in PEDTT. From the features in MC, a magnetic transition occurs. This should be further investigated in the context of magnetic susceptibility measurements such as vibrating sample magnetometry (VSM) or AC-susceptibility measurements. Results indicate that PEDTT:sulphate is not only a conductive polymer but also presents an interesting spin-system.

However, conceptually this is as far as structural stabilization in PEDTT can go without growing it into a well engineered and defined surface-structure. A possibility for further improvement might lie in further optimization of the deposition process and in a careful choice of the substrate. A concept suggested to me by Prof. Michael L. Hitchman was the use of a low-pressure system instead of working in a gas flow at ambient pressures. This should achieve more uniform coatings and would allow for more efficient use of the reaction materials. However, the question would remain, if such a step would not take away the advantage of an intrinsic cleaning step that is present in the GC-like principle of our CVD-system.

With PTP, we did not achieve high conductivity, in fact, the source of the conductivity of 0.5 S/cm measured is highly questionable. Results from XPS and its behaviour during conductivity measurements suggest it to be a highly porous system filled with electrolyte. However, an important lesson can be learned in the synthesis process: the presence of nitrogen in a conductive polymer will lead to strong interactions to glass, which for industrial processes can present an important advantage. Combined with a CP like PEDOT:sulphate, a layer of PTP of a few nm could well be used to achieve highly conductive systems with extraordinary adhesion to glass.

Another interesting application might lie in the use of PTP in the context of $CO_2$ reduction. The presence of an amine being able to bind the gas-molecules in order to be reduced.[18]

For closing words, sulphate based oCVD presents an important contribution to the field and presents an extraordinary tool for advances in solid state physics: simple chemistry and simple handling delivering high-end materials.

In terms of applications, the situation might be different. Presently, I see the use of sulphate-doped CP's in a niche application, only. These would be in fields where oxidation-resistant conducting systems are prerequisite. A possible way how to make these materials more interesting would be the development of an interlayer that would contain sulphate-ions within the polymer matrix.

Personally, I value the work of the last years as highly rewarding, both scientifically as personally. I was able to develop my skills related to chemistry and to the characterization of electron transport phenomena in the solid state. As a consequence of my work I had the chance to speak and discuss with Nobel laureates and great minds of today and tomorrow. This thesis was a challenge beyond the scientific.

## 9. Literature

[1] C.K. Chiang, C.R. Fincher, Y.W. Park, A.J. Heeger, H. Shirakawa, E.J. Louis, S.C. Gau, and A.G. MacDiarmid, Phys. Rev. Lett. **39**, 1098 (1977).

[2] H. Shirakawa, E.J. Louis, A.G. MacDiarmid, C.K. Chiang, and A.J. Heeger, J. Chem. Soc. Chem. Commun. 578 (1977).

[3] R. Menon, Synth. Met. **80**, 223 (1996).

[4] M. Ahlskog and M. Reghu, J. Phys. Condens. Matter **101**, 6779 (1998).

[5] J. Plocharski, W. Pukacki, and S. Roth, J. Polym. Sci. Part B Polym. Phys. **32**, 447 (1994).

[6] D. Farka, H. Coskun, J. Gasiorowski, C. Cobet, K. Hingerl, L.M. Uiberlacker, S. Hild, T. Greunz, D. Stifter, N.S. Sariciftci, R. Menon, W. Schoefberger, C.C. Mardare, A.W. Hassel, C. Schwarzinger, M.C. Scharber, and P. Stadler, Adv. Electron. Mater. (2017).

[7] B.J. Worfolk, S.C. Andrews, S. Park, J. Reinspach, N. Liu, M.F. Toney, S.C.B. Mannsfeld, and Z. Bao, Proc. Natl. Acad. Sci. **112**, 14138 (2015).

[8] O. Bubnova, Z.U. Khan, H. Wang, S. Braun, D.R. Evans, M. Fabretto, P. Hojati-Talemi, D. Dagnelund, J.-B. Arlin, Y.H. Geerts, S. Desbief, D.W. Breiby, J.W. Andreasen, R. Lazzaroni, W.M. Chen, I. Zozoulenko, M. Fahlman, P.J. Murphy, M. Berggren, and X. Crispin, Nat. Mater. **13**, 190 (2013).

[9] N. Massonnet, A. Carella, A. de Geyer, J. Faure-Vincent, and J.-P. Simonato, Chem. Sci. **6**, 412 (2015).

[10] M.N. Gueye, A. Carella, N. Massonnet, E. Yvenou, S. Brenet, J. Faure-Vincent, S. Pouget, F. Rieutord, H. Okuno, A. Benayad, R. Demadrille, and J.P. Simonato, Chem. Mater. **28**, 3462 (2016).

[11] D. Farka, H. Coskun, P. Bauer, D. Roth, B. Bruckner, P. Klapetek, N.S.S. Sariciftci, and P. Stadler, Monatshefte Fur Chemie **148**, 871 (2017).

[12] R.P. Fornari, P.W.M. Blom, and A. Troisi, Phys. Rev. Lett. **118**, 86601 (2017).

[13] S.K.M. Jönsson, J. Birgerson, X. Crispin, G. Greczynski, W. Osikowicz, A.W. Denier van der Gon, W.R. Salaneck, and M. Fahlman, Synth. Met. **139**, 1 (2003).

[14] C.M. Palumbiny, F. Liu, T.P. Russell, A. Hexemer, C. Wang, and P. Müller-Buschbaum, Adv. Mater. **27**, 3391 (2015).

[15] Z. Yu, Y. Xia, D. Du, and J. Ouyang, ACS Appl. Mater. Interfaces **8**, 11629 (2016).

[16] T. Stöcker, A. Köhler, and R. Moos, J. Polym. Sci. Part B Polym. Phys. **50**, 976 (2012).

[17] T.-R. Chou, S.-H. Chen, Y.-T. Chiang, Y.-T. Lin, and C.-Y. Chao, J. Mater. Chem. C **3**, 3760 (2015).

[18] H. Coskun, A. Aljabour, P. De Luna, D. Farka, T. Greunz, D. Stifter, M. Kus, X. Zheng, M. Liu, A.W. Hassel, W. Schöfberger, E.H. Sargent, N.S. Sariciftci, and P. Stadler, Sci. Adv. **3**, (2017).

[19] H. Coskun, A. Aljabour, L. Uiberlacker, M. Strobel, S. Hild, C. Cobet, D. Farka, P. Stadler, and N.S. Sariciftci, Thin Solid Films **645**, 320 (2018).

[20] S. Lee, D.C. Paine, and K.K. Gleason, Adv. Funct. Mater. **24**, 7187 (2014).

[21] A.M. Coclite, R.M. Howden, D.C. Borrelli, C.D. Petruczok, R. Yang, J.L. Yagüe, A. Ugur, N. Chen, S. Lee, W.J. Jo, A. Liu, X. Wang, and K.K. Gleason, Adv. Mater. **25**, 5392 (2013).

[22] A. Ugur, F. Katmis, M. Li, L. Wu, Y. Zhu, K.K. Varanasi, and K.K. Gleason, Adv. Mater. **27**, 4604 (2015).

[23] E.D. Głowacki, G. Voss, K. Demirak, M. Havlicek, N. Sünger, A.C. Okur, U. Monkowius, J. Gąsiorowski, L. Leonat, and N.S. Sariciftci, Chem. Commun. **49**, 6063 (2013).

[24] D . J . T h o u l e s s, J. Non. Cryst. Solids **35&36**, 3 (1980).

[25] G.D. Christian, P.K. Dasgupta, and K.A. Schug, *Analytical Chemistry* (2013).

[26] C. Kvarnström, A. Ivaska, and H. Neugebauer, in *Adaanced Funct. Mol. Polym.* (200AD), pp. 139–170.

[27] K. Hinrichs, K.J. Eichhorn, G. Ertl, D.L. Mills, and H. Lüth, *Ellipsometry of Functional Organic Surfaces and Films* (2014).

[28] H.G. Tompkins and E.A. Irene, *Handbook of Ellipsometry* (2005).

[29] R.A. Synowicki, Phys. Status Solidi Curr. Top. Solid State Phys. **5**, 1085 (2008).

[30] in *Nanoscopic Mater. Size-Dependent Phenom.* (2006), pp. 11–20.

[31] M. Tolan, *X-Ray Scattering from Soft-Matter Thin Films: Materials Science and Basic Research* (1998).

[32] D. Briggs, in *Cambridge, UK Cambridge Univ. Press* (1998), p. 198.

[33] R. Steinberger, J. Duchoslav, T. Greunz, M. Arndt, and D. Stifter, Corros. Sci. **90**, 562 (2015).

[34] T. Greunz, H. Duchaczek, R. Sagl, J. Duchoslav, R. Steinberger, B. Strauß, and D. Stifter,

Appl. Surf. Sci. **396**, 665 (2017).

[35] I. Solomon, J. Optoelectron. Adv. Mater. **4**, 419 (2002).

[36] N.F. Mott, *Metal-Insulator Transitions*, 1st ed. (Taylor & Francis LTD, London, 1974).

[37] D. Belitz and T.R. Kirkpatrick, Rev. Mod. Phys. **66**, 261 (1994).

[38] N.E. Hussey, K. Takenaka, and H. Takagi, Philos. Mag. **84**, 2847 (2004).

[39] S.N. Mott, Phys. Today **31**, 42 (1978).

[40] K. Sato, M. Yamaura, T. Hagiwara, K. Murata, and M. Tokumoto, Synth. Met. **40**, 35 (1991).

[41] J. Roncali, Macromol. Rapid Commun. **28**, 1761 (2007).

[42] P. Blanchard, A. Cappon, E. Levillain, Y. Nicolas, P. Frère, and J. Roncali, Org. Lett. **4**, 607 (2002).

[43] J. Roncali, Chem. Rev. **97**, 173 (1997).

[44] J.H. Kim, H.K. Sung, C.O. Yoon, H. Lee, K.C. Laboratories, K. Kumho, P. Company, and S. Korea, **84**, 737 (1997).

[45] J.H. Mooij, Phys. Status Solidi **17**, 521 (1973).

[46] D. Joung and S.I. Khondaker, Phys. Rev. B **86**, 235423 (2012).

[47] A.B. Kaiser and V. Skákalová, Chem. Soc. Rev. **40**, 3786 (2011).

[48] S.D. Baranovskii, Phys. Status Solidi Basic Res. **251**, 487 (2014).

[49] N.F. Mott, Rev. Mod. Phys. **40**, 677 (1968).

[50] A.G. Zabrodskii and K.N. Zinov'eva, Zh. Eksp. Teor. Fiz. **86**, 727 (1984).

[51] A.G. Zabrodskii, Physics-Uspekhi **41**, 722 (1998).

[52] A.B. Kaiser, Reports Prog. Phys. **64**, 1 (2001).

[53] R. Menon, K. Väkiparta, Y. Cao, and D. Moses, Phys. Rev. B **49**, 16162 (1994).

[54] G. Bergmann, Phys. Rev. B **28**, 2914 (1983).

[55] G. Bergmann, Physica **126B**, 229 (1984).

[56] T.F. Rosenbaum, R.F. Miligan, G.A. Thomas, P.A. Lee, T.V. Ramakrishnan, R.N. Bhatt, H. DeConde, K., Hess, and T. Perry, Phys. Rev. Lett. **47**, 1758 (1981).

[57] A. Kawabata, Solid State Commun. **34**, 431 (1980).

[58] Jaiswal, Manu and R. Menon, Polym. Int. **55**, 1371 (2006).

[59] C. Ohashi, S. Izawa, Y. Shinmura, M. Kikuchi, S. Watase, M. Izaki, H. Naito, and M. Hiramoto, Adv. Mater. **29**, (2017).

[60] J.W. Orton and M.J. Powell, Reports Prog. Phys. **43**, 1263 (1980).

[61] K. Murata, K. Yokogawa, S. Arumugam, and H. Yoshino, Crystals **2**, 1460 (2012).

[62] M.J. Clark and T.F. Smith, J. Low Temp. Phys. **32**, 495 (1978).

[63] S. Masubuchi, S Fukuhara, T, Kazama, Synth. Met. **84**, (1997).

[64] R. Menon, C.O. Yoon, D. Moses, Y. Cao, and A.J. Heeger, Synth. Met. **69**, 329 (1995).

[65] S.G. Duyker, V.K. Peterson, G.J. Kearley, A.J. Studer, and C.J. Kepert, Nat. Chem. **8**, 270 (2016).

[66] E. Magos-Palasyuk, K.J. Fijalkowski, and T. Palasyuk, Sci. Rep. **6**, 28745 (2016).

[67] S.O. Dwyer, H. Xie, M. Knaapila, and S. Guha, J. Phys. Condens. Matter **10**, 7145 (1998).

[68] K. Yokogawa, K. Murata, H. Yoshino, and S. Aoyama, Jpn. J. Appl. Phys. **46**, 3636 (2007).

[69] J. Hynynen, D. Kiefer, L. Yu, R. Kroon, R. Munir, A. Amassian, M. Kemerink, and C. Müller, Macromolecules **50**, 8140 (2017).

[70] G. Conboy, H.J. Spencer, E. Angioni, A.L. Kanibolotsky, N.J. Findlay, S.J. Coles, C. Wilson, M.B. Pitak, C. Risko, V. Coropceanu, J.-L. Brédas, and P.J. Skabara, Mater. Horiz. **3**, 333 (2016).

[71] D. Farka, A.O.F. Jones, R. Menon, N.S. Sariciftci, and P. Stadler, Synth. Met. **240**, 59 (2018).

[72] A.A. Farah, S.A. Rutledge, A. Schaarschmidt, R. Lai, J.P. Freedman, and A.S. Helmy, J. Appl. Phys. **112**, 113709 (2012).

[73] E.J. Bae, Y.H. Kang, K. Jang, and S.Y. Cho, Nat. Publ. Gr. 1 (2016).

[74] P.A. Lee and T. V. Ramakrishnan, Rev. Mod. Phys. **57**, 287 (1985).

[75] A.B. Kaiser, Synth. Met. **45**, 183 (1991).

[76] A.N. Aleshin and R. Kiebooms, Synth. Met. **101**, 369 (1999).

[77] M. Ahlskog, M. Reghu, and A.J. Heeger, J. Phys. Condens. Matter **9**, 4145 (1997).

[78] C. Wang, J.L. Schindler, C.R. Kannewurf, and M.G. Kanatzidis, Chem. Mater. **7**, 58 (1995).

[79] D. Farka, T. Greunz, D. Stifter, C.C. Mardare, C. Cobet, N.S. Sariciftci, and P. Stadler, Prep. **In prepara**, In preparation (n.d.).

[80] J. Kastner, H. Kuzmany, D. Vegh, M. Landl, L. Cuff, and M. Kertesz, Synth. Met. **69**, 593 (1995).

[81] S.C. Rasmussen, D.D. Kenning, M.R. Funfar, S.C. Rasmussen, K.A. Mitchell, T.R. Calhoun, M.R. Funfar, D.J. Sattler, and S.C. Rasmussen, J. Org. Chem. **67**, 9073 (2002).

[82] O. Kwon and M.L. McKee, J. Phys. Chem. A **104**, 7106 (2000).

[83] S.C. Rasmussen, D.D. Kenning, M.R. Funfar, and S.C. Rasmussen, Polym. Prepr. **42**, 506 (2001).

[84] R. Mondal, S. Ko, and Z. Bao, J. Mater. Chem. **20**, 10568 (2010).

[85] Cheng, Kai-Fang, Liu, Cheng-Liang, and W.-C. Chen, J. Polym. Sci. Part A Polym. Chem. **45**, 5872 (2007).

[86] H. Coskun, A. Aljabour, P. De Luna, D. Farka, T. Greunz, D. Stifter, M. Kus, X. Zheng, M. Liu, A.W. Hassel, W. Schöfberger, E.H. Sargent, N.S. Sariciftci, and P. Stadler, Sci. Adv. **3**, (2017).

[87] D. Farka, T. Greunz, D. Stifter, N.S. Sariciftci, and P. Stadler, Prep. **In prepara**, In preparation (n.d.).

## 10. Funding

## 11.  Curriculum vitae

Dominik Farka
Address: Julius-Raab-Straße 5-7
4040 Linz, Austria
Contact:
tel.: +43 (0) 699 11 98 27 53
Email: dominik.farka@jku.at
Date of Birth: 12.1.1990
Place of Birth: Vienna, Austria
Nationality: Austrian, Czech

### EDUCATION

| | |
|---|---|
| 4/2015-now | Study of PhD programme in Natural Sciences at Johannes Kepler University (Linz, Austria) |
| 10/2012- 3/2015 | Study of master curriculum „Joint Master Programme: Biological Chemistry" at Johannes Kepler University (Linz, Austria) and University of South Bohemia (Budweis, Czech Republic) |
| 10/2009-6/2012 | Study of bachelor curriculum „Biological Chemistry" at Johannes Kepler University (Linz, Austria) and University of South Bohemia (Budweis, Czech Republic) |
| 10/2004-6/2008 | „Bilinguales Oberstufenrealgymnasium Komensky", Vienna (with emphasis on mathematics and descriptive geometry) |

### WORK EXPERIENCE

| | |
|---|---|
| 02/2018 | Research Stay at the Lawrence Berkeley National Lab, California, USA |
| 04/2015-03/2018 | PhD thesis at Linz Institute of Organic Solar Cells |
| 09/2014-03/2015 | Master thesis at Linz Institute of Organic Solar Cells |
| 04/2014-07/2014 | Internship at Linz Institute of Organic Solar Cells |
| 07/2013-08/2013 | Internship at Linz Institute of Organic Solar Cells |
| 09/2012-01/2013 | Internship at the Institute of Nanobiology and Structural Biology (Czech Academy of Sciences) and at the Institute of Physical Chemistry (Czech Academy of Sciences) |
| 09/2011 | Bachelor thesis (2nd thesis) at Institute of Inorganic Chemistry (Center for Nanobionics and Photochemical Sciences) |
| 08/2011 | Internship at the "Austrian Agency for Health and Food Safety (AGES)" (Center of Competence: Biochemistry) |
| 05/2010-07/2011 | Bachelor thesis at the Laboratory of Nematology, Institute of Parasitology (Czech Academy of Sciences) |
| 12/2010-04/2011 | Internship at the Laboratory of Nematology, Institute of Parasitology (Czech Academy of Sciences) |
| 08/2010 | Internship at the "Austrian Agency for Health and Food Safety (AGES)" (Institute of Plant Variety) |

| | | |
|---|---|---|
| 10/2008- 03/2009 | Compulsory basic military service including posting to the Austrian-Slowakian border (medic- training completed) |
| 10/2006-08/2008 | Journalist and moderator at the Austrian Broadcasting Corporation (ORF) Radio 1476 (for the weekly broadcasting of the Czech minority programme "Rádio Zvídavý Mikrofon") |
| 09/2008 | Internship at "Karasek Wietrzyk Rechtsanwälte" (law firm with focus on business law) |
| 08/2007 | Internship at "Karasek Wietrzyk Rechtsanwälte" (law firm with focus on business law) |
| 08/2006 | Internship at "Karasek Wietrzyk Rechtsanwälte" (law firm with focus on business law) |

## LANGUAGES

| | A1 | A2 | B1 | B2 | C1 | C2 |
|---|---|---|---|---|---|---|
| German | | | | | | Mother tongue |
| Czech | | | | | | Second mother tongue |
| English | | | | | | |
| French | | | Learning | | | |
| Russian | | | | | | |
| Japanese | | | | | | |
| Slowak | | | | | | |

## THESES

Doctoral Thesis    (pending)
Title:    Conductive, (semi)-transparent, metallic polymers
Supervisor:    o. Univ. Prof. Mag. Dr. DDr. h.c. Niyazi Serdar Sariciftci

Masterthesis
Title:    Spectroscopic Investigation of Luminescent Biomaterials on Organic Semiconductors
Supervisor:    o. Univ. Prof. Mag. Dr. DDr. h.c. Niyazi Serdar Sariciftci
Sec. Supervisor:    Dr. Eric Głowacki, MSc

Bachelorthesis #1
Title:    Titration of Human Serum Albumin and Human Transferrin with Water-Soluble Corroles
Supervisor:    Assoc. Univ.-Prof. Dr. Wolfgang Schöfberger

Bachelorthesis #2
Title:    Making Transgenic *C. Elegans* with Polycistronic mCherry Vector
Supervisor:    Dr. Masako Asahina-Jindrová, PhD

## ADDITIONAL SKILLS

Driving licence (B)
Passive knowledge of programming languages Java and Perl
Programmes: Microsoft Office, Origin, Sketchup, Complete EASE
Social skill due to service as a medic, journalistic work, and two terms as head boy

## SCIENTIFIC CONTRIBUTIONS

**Talks and Poster Presentations:**

**Scientific Talk:** Molecular Foundry, Lawrence Berkeley National Lab, "Leaping Disorder - Towards Metallic, Conducitve Polymers" (Berkeley. California, USA; February 2018)

**Scientific Talk:** 10 years Biological Chemistry symposium, "Beyond Biology" (Linz. Austria; October 2017)

**Scientific Talk:** Chemietage 2017 (meeting of the Austrian Chemical Society) "Overcoming Disorder in PEDOT:sulphate" (Salzburg. Austria; September 2017)

**Scientific Talk:** European Materials Research Society "Indium-free transparent electrodes made of highly conductive PEDOT:sulphate using CVD method" (Warsaw. Poland; September 2017)

**Scientific Pitch:** 67th Lindau Nobel Laureate Meeting at the Bayer Science Foundations Science Pitch (Lindau, Germany; July 2017)

**Scientific Talk:** European Materials Research Society "PEDOT:sulphate: A Conductive, Semitransparent Polymer Metal" (Warsaw. Poland; September 2016)

**Poster Presentation:** International Symposium for the 80th Birthday of Prof. Alan J. Heeger (Linz, Austria; March 2016)

**Scientific Talk:** Materials Research Society Student Chapter Vermont: "Bioconjugation of Hydrogen-Bonded Organic Semiconductors with Functional Proteins" (Burlington, USA; December 2015)

**Scientific Talk:** Materials Research Society Fall Meeting 2015 (Symposium D): "Bioconjugation of Hydrogen-Bonded Organic Semiconductors with Functional Proteins" (Boston, USA; November/December 2015)

**Poster Presentation:** International Winterschool on Bioelectronics (Kirchberg, Austria; February/March 2014)

**Poster presentation:** International Winterschool on Bioelectronics (Kirchberg Austria, February/March 2014)


**Publications:**

Farka D, Jones AOF, Menon R, Sariciftci NS, Stadler P, Metallic conductivity beyond the Mott minimum in PEDOT:sulphate at low temperatures, accepted at *Synthetic Metals*

Coskun H, Aljabour A, Uiberlacker L, Strobel M, Hild S, Cobet C, Farka D, Stadler P, Sariciftci NS, Chemical vapor deposition-based synthesis of conductive polydopamine thin-films, *Thin Solid Films*, **2018**, 645, 320-325

Coskun H, Aljabour A, Luna PD, Farka D, Greunz T, Stifter D, Kus M, Zheng X, Liu M, Hassel AW, Schöfberger W, Sargent EH, Sariciftci NS, Stadler P; Biofunctionalized conductive polymers enable efficient $CO_2$ electroreduction; *Science Advances*, **2017**, 3, 8, e1700686

Farka D, Coskun H, Bauer P, Roth D, Bruckner B, Klapetek P, Sariciftci NS, Stadler P; Increase in electron scattering length in PEDOT:PSS by triflic acid post-processing; **2017**, *Monatshefte für Chemie- Chemical Monthly*, 148, 5, 871-877

Farka D, Coskun H, Gasiorowski J, Cobet C, Hingerl K, Uibelacker LM, Hild S, Greunz T, Stifter D, Sariciftci NS, Menon R, Schoefberger W, Madrare CC, Hassel AW, Schwarzinger C, Scharber MC, Stadler P; Anderson localization and the Mott-Ioffe-Regel limit in glassy-metallic PEDOT; **2017**, *Advanced Electronic Materials*, 1700050

Stadler P, Farka D, Coskun H, Głowacki ED, Yumusak C, Uiberlacker LM, Hild S, Leonata LN, Scharber MC, Klapetek P, Menon R, Sariciftci NS; Local Order Drives the Metallic State in PEDOT:PSS; *Journal of Material Chemistry C*; **2016**, Advance Article DOI: 10.1039/c6tc02129h

Głowacki ED, Tangorra RR, Coskun H, Farka D, Operamolla A, Kanbur Y, Milano F, Giotta L, Farinola GM, Sariciftci NS; Bioconjugation of Hydrogen-Bonded Organic Semiconductors with Functional Proteins; *Journal of Material Chemistry C;*, **2015,** 3, 6554-6564

Farka D, Scharber M, Głowacki ED, Sariciftci NS; Reversible Photochemical Isomerisation of *N,N*-di(*t*-butoxycarbonyl)indigos; *Journal of Physical Chemistry A*, **2015**, *119* (15), 3563-3568

## Achievements and Scholarships

| | |
|---|---|
| February 2018 | Affiliate at the Lawrence Berkeley National Lab (sponsorships acquired from the State of Upper Austria and the "Österreichische Forschungs Gemeinschaft") |

| July 2017 | giving an interview for the Austrian Broadcasting Agency (ORF) related to the participation at the "67th Lindau Nobel Laureate-meeting" |
|---|---|
| July 2017 | selected as one of 20 scientists for the annual post conference programme of the "Lindau Nobel Laureate-meeting", organized by Baden-Württemberg International |
| June 2017 | selected as one of 400 scientists for participation at the "67th Lindau Nobel Laureate Meeting" dedicated to the field of chemistry |
| November 2015 | Symposium Assistant Materials Research Society (MRS) Fall Meeting 2015 Boston |
| February 2014 | Students Scholarship: International Winterschool on Bioelectronics |

## Memberships

Student member of the Austrian Chemical Society (GÖCH)

Member of the Critical Raw Materials COST action (CRM-extreme COST)

## INTERESTS

Music, literature, learning languages, hiking, travelling, painting, crafting, gardening;